806 February 24, 1999

Equation of state for a partially ionized gas

George A. Baker, Jr.

Theoretical Division, Los Alamos National Laboratory

University of California, Los Alamos, N. M. 87544 USA

(10 June 1997)

Abstract

The derivation of equations of state for fluid phases of a partially ionized gas or plasma is addressed from a fundamental point of view. First, a cubic cellular model and then a spherical cellular model is deduced for the hot curve limit (or ideal Fermi gas). Next the Coulomb interactions are added to the spherical model for general ionic charge Z. A numerical example of the theory for the case of hydrogen is reported and it reduces in various limits of temperature and density to the expected behavior. It displays an electron, localization-delocalization phase transition of the normal liquid-gas character.
05.30.-d, 51.30.+i,05.70.-a,64.70.Fx

Typeset using REVTEX

I. INTRODUCTION AND SUMMARY

The theory of crystalline solids is currently very well developed and relies on Bloch's theorem to provide the structure of the necessary quantum mechanical wave functions. This theory has been successfully investigated in great detail by numerous workers. The properties of fluids and amorphous solids, considered at the correspoding level of their basic constituents, *i.e.,* electrons and ions, has received very much less attention. It is the purpose of this paper to begin an effort to construct such a fundamental investigation of the problem of the partially ionized gas. Needless to say there is no clear dividing line between partially ionized, and fully ionized, nor for that matter, non-ionized. The resulting model has been evaluated in the case of hydrogen, and the results have all the expected physical properties. The limiting pressure is correct for high temperature. The model shows the expected complete ionization phenomena for fixed temperature in the dilute limit. As expected at medium to high densities, the model predicts a "cold curve" where the pressure is very insensitive to the temperature. (The compression pressure dominates.) It also predicts a localization-delocalization phase transition, although critical parameters are not yet in accord with experimental results.

Perhaps the theories in most general use today are the Thomas-Fermi [1–6] and Thomas-Fermi-Dirac theories [7,8]. These theories permit the computation of the equations of state over wide regions of temperature and volume, however they are basically semi-classical in nature.

There are a number of other approaches which have been employed, many of which are quite good in certain regions of the phase diagram. There is the classical theory of ionic fluids of Debye-Hückel [9]. A more modern version of it is the restricted primitive model [10,11]. In this model there is a fifty-fifty mixture of hard spheres with charges $+q$ and $-q$, which move in a dielectric medium. This model is suitable for Monte Carlo simulations and for mean-field approximations. It produces results which compare informatively [12] with experimental data. The hard-sphere reference system for the neutral components has also

been used [13,14]. The thermodynamic perturbation theory approach in its classical [15,16] and quantum [17,18] forms has been used. In addition there is the perturbation expansion in the electric charge [19]. A further approach which has been very thoroughly worked out is to use an empirical interatom potential. The Lenard-Jones 6-12 potential (sometimes cut off at larger distances) is a popular choice. Rather full results have been obtained here for the equation of state [20–22]. There is the method of Bunker *et al.* [23] who is concerned with the metalization of hydrogen. It uses fluid variational theory, a modified hyper-netted chain approach, and empirical species-species potentials. A description of a number of additional approaches may be found in the book Kraeft *et al.* [24], plus some subsequent work which takes into account some of the many-body effects (dynamical screening, self energy, and polarization forces) [25,26].

An approach somewhat similar to the present approach is the confined atom method [27,28]. It differs from our current method, and my report of some preliminary results from a precursor to the present method [29], by requiring for all angular momentum states that the wave function vanish at the cell boundaries. It is well known that for these boundary conditions that the lowest eigenvalue is never less than that for the atom, whereas in the case of the present approach the lowest eigenvalue may well be lower [30] in a manner similar to the so called "metallic bond." A first principles type of approach is the quantum Monte Carlo method which has been applied to a system of 32 electrons and 32 protons, with the observation of phase transition [31].

Our alternate approach is to start from the ideal electron gas plus a gas of ions, all of which are non-interacting. This system corresponds to a state of complete ionization. It represents the correct description when the electric charge e is set to zero. The deviations from complete ionization by means of many-body perturbation theory in the electric charge (or more accurately in terms of e^2) have been studied for some time. The leading correction is the exchange correction [7] as all the direct terms cancel each other for the case of charge neutrality. The next correction is the Debye-Hückel term which is of order e^3 and results from the sum of an infinite series of terms of order e^4 [32]. The term of order e^4, the

second exchange correction, was added by Baker and Johnson [19]. This approach is plainly completely correct within its region of validity. The requirement for its validity is the smallness of the Coulomb interaction relative to the thermal energy. This approach is quite good for large temperatures and/or high densities.

In this paper we apply a number of the insights gained by the study of crystalline solids to an effort to construct a theory of quantum fluid behavior. The cellular model is an old idea [33] in that theory. For crystals, the cells can be chosen so that space is completely filled, opposite sides have values of the wave function related by the lattice periodicity. I will apply the idea of a cellular model to the case of a fluid. For a fluid, there is no preferred direction, so that one is force to choose a spherical cell. Since one can not fill space with spheres of uniform diameter, as one could with Wigner-Seitz cells, this choice is necessarily an approximate one. Various many-body effects are added to the spherical cell model through the boundary conditions, an effective mass, and changes to the potential.

In the second section of this paper I give the derivation of the Schrödinger equation for our case. I also outline the necessary thermodynamics and statistical mechanics to compute the pressure, internal energy, *etc.* for our case. Some care must be taken here as our case is a more general one than is often seen.

In the third section, I show how to construct a cellular model of the ideal Fermi gas. Here cubic cells are used and the model is in principle exact for this case. Some discussion is given regarding the various integrals over the Brillouin zone which need to be evaluated. This model is evaluated numerically. I show how to obtain the fugacity in this case. The results are found to be in agreement with the exact ones, as expected.

In the fourth section I construct a spherical cellular model of the ideal Fermi gas. I discuss the question of the selection of appropriate boundary conditions. In addition to the problem of spheres not filling space, there is an additional problem which arises. We resolve the wave function in the usual spherical coordinates, and then we let l denote the angular momentum index and λ the radial wave function index. In the Hamiltonian there is a term $\vec{k} \cdot \vec{\nabla}$, where $\vec{k}$ is a vector in the Brillioun zone. This term unfortunately couples

components with all values of λ to the components with adjacent values of l. This problem greatly complicates the numerical work. I have used the observation of the degeneracy and near degeneracy of the eigenvalues to give a prescription to reduce this numerical problem to a more tractable level. As a result, the pressure as computed by this method is accurate to within -2.5 to $+4.9$ percent.

In the fifth section, we come to the heart of the paper. Here I show how to construct a spherical cellular model of an ion-electron gas. I begin with a simplified discussion of the cases of hydrogen. I start with the Heitler-London atom. Drawing on our knowledge of the high-temperature limit, the electron-ion, electron-electron, and ion-ion interactions are adjusted to lead to correct results in that case. A modification of the various potentials is used to this end. Next the exchange correction is considered and an effective mass term is introduced as well as a further potential modification. Again our knowledge of the high temperature limit is used to guide the construction of these modification. Finally a correction of a semi-classical nature is made to take account of the fact that the electron-electron and ion-ion repulsions forces the electrons apart and so reduces the energies which depend on these interactions. These resulting equations are then generalized to general nuclear charge Z together with Z surrounding electrons.

In the last section, I compute the results of the spherical cellular model for the case of hydrogen. The results are as described above.

II. GENERAL FORMALISM FOR THE CELLULAR MODEL OF A GAS

Our work here will be based on the independent electron approximation, modified as appropriate to included further important effects. That approximation is certainly generally valid for an ideal Fermi gas, and we also expect it to be very good for the application to extremely low density atomic hydrogen. In the absence of other, more reliable, pictures we shall be guided here by the way in which this approximation is structured for a crystal, while keeping in mind that what we are doing should work for an ideal Fermi gas. From a

fundamental point of view, it is impossible to describe the behavior of the electrons correctly in terms of the solutions of a one electron Schrödinger equation, no matter how cleverly the potential, *etc.* is chosen. Never-the-less, the independent electron approximation has had very considerable success in the theory of crystalline solids. If we make this approximation, then we expect to represent the crystal by a periodic lattice of ions which leads in turn to a periodic potential. The solutions for the single electron wave functions in this case can by Bloch's theorem be represented in terms of the wave function in a single lattice cell and a wave vector in the first Brillouin zone. The difficulty in determining the appropriate potential within the cell is well known. In the case of a fluid it may seem jarring, to those who are used to thinking of a fluid as a many body system in continuous space, to discretize the system by dividing it up into cells. However, following the Wigner-Seitz construction, if we take a given configuration of ions and put a surface half way between each ion and its nearest neighbor ions, we will divide the system into cells of various sizes and shapes with one ion in the 'center' of each cell. As the ions are much heavier than the electrons, we expect the electrons to relax into configurations in these cells on a time scale shorter than that of the movement of the ions. In the independent electron approximation, we generate the energy states of the system by the use of the eigenfunctions of the single electron interacting via an appropriate potential in each of these cells, just as was done in the crystal case. Rather that treat such an ensemble of different cell types, in this effort we replace them by a single cell whose volume is equal to the average volume. To the extent that volume fluctuations are important, they are ignored here. This uniformization of cell size allows us, as in the crystal case, reasonably to suppose that we can describe the system in terms of the eigenvalues of the solution within a single cell and the wave vectors of the first Brillouin zone. The eigenspectrum of the individual cell, together with the spread in these energy levels due the the wave vectors just mentioned, models (in the independent electron approximation) the energy eigenspectrum of the whole system. We will see in the next section that this method is exactly correct for a cubic cell model of the ideal gas. Further, we know from tight-binding approximation theory that, at least for the low-lying levels, it is very accurate in the cold

dilute limit of an interacting Coulomb system. That the model behaves correctly in these two extremes is a necessary, but not a sufficient condition for its over all validity. Our choice of what seems to be a reasonable intra-cellular potential is addressed in section V. The issue of the screening of the electric charges is handled in this model by the enforced neutrality of each cell. If the electronic state is spherically symmetric, then the force outside the cell is zero. Otherwise, higher-order moment forces can occur. The cell-cell interaction forces are modeled here, as we will see later, by means of the boundary conditions. As explained in section V this model, in some sense, replaces the long-range part of the potential by a nearest-neighbor, cell-cell interaction.

The first step is to divide the system up into Wigner-Seitz cells, with one atom per cell. We will not specify the underlying lattice now, but will choose it later to fit our convenience. We will however insist that the Wigner-Seitz cells chosen be inversion invariant. Bloch's theorem on crystal lattices [6] says that any solution for the "one-electron wave function" is of the form $\psi(\vec{r}) = e^{i\vec{k}\cdot\vec{r}}\phi(\vec{r})$, where $\phi(\vec{r})$ has the periodicity of the lattice. By using all the $\vec{k}$ which lie in the first Brillouin zone, one can construct the entire band corresponding to that state. By the general theory the combination of all the reciprocal lattice vectors plus those in the first Brillouin zone covers the entire $\vec{k}$-space. We will see later that our procedures will allow us to construct a correct model of an ideal gas. Although this procedure is more complex than the standard one, it can be generalized to the non-ideal case more readily. The point is not to construct a band theory of a gas, but rather to use this method to include the Pauli exclusion principle effects between electrons on different atoms. We add that to the extent that shape fluctuations are important, they are ignored in this procedure. Here the boundary conditions are

$$\psi(\vec{r}) = e^{-i\vec{k}\cdot\vec{R}}\psi(\vec{r}+\vec{R}) \tag{2.1}$$

and

$$\vec{n}(\vec{r})\cdot\vec{\nabla}\psi(\vec{r}) = -e^{-i\vec{k}\cdot\vec{R}}\vec{n}(\vec{r}+\vec{R})\cdot\vec{\nabla}\psi(\vec{r}+\vec{R}), \text{ or } \vec{n}(\vec{r})\cdot\vec{\nabla}\phi(\vec{r}) = -\vec{n}(\vec{r}+\vec{R})\cdot\vec{\nabla}\phi(\vec{r}+\vec{R}), \tag{2.2}$$

where $\vec{n}(\vec{r})$ is the outward normal vector to the surface of the cell and $\vec{R}$ is a lattice vector. These conditions provide for the continuity of the wave function and its derivative at the surface of the cell. From our point of view, every calculation we make must be reduced to a single cell and the macroscopic effects are reflected solely through the boundary conditions, and the effective mass and potential modifications.

The next step is to substitute $e^{i\vec{k}\cdot\vec{r}}\phi_\lambda(\vec{r})$ into the Schrödinger equation.

$$\frac{\hbar^2 k^2}{2m}\phi_\lambda(\vec{r}) - \frac{i\hbar^2}{m}\vec{k}\cdot\vec{\nabla}\phi_\lambda(\vec{r}) - \frac{\hbar^2}{2m}\nabla^2\phi_\lambda(\vec{r}) + V(\vec{r})\phi_\lambda(\vec{r}) = E_\lambda(\vec{k})\phi_\lambda(\vec{r}). \tag{2.3}$$

Of course the issue of the best choice of $V(\vec{r})$ is an important one, and we shall return to this topic in section V. We will however use an inversion invariant potential. Notice that the left-hand side of (2.3) is Hermitian, so $E_\lambda(\vec{k})$ is necessarily real. Note also that since the Wigner-Seitz cell is inversion invariant and (2.3) is invariant under inversion and complex conjugation, it must be that if $\phi_\lambda(\vec{r})$ is an eigenfunction, then so too is $\phi^*_\lambda(-\vec{r})$. If the eigenvalue is non-degenerate then these two quantities must be a constant multiple of each other.

Next we need the pressure of an atom enclosed in a cell. We will suppose that the nucleus is fixed in the center of the cell. The most straightforward thing to compute is the grand canonical partition function which is normally given as [34]

$$\begin{aligned}\mathcal{Q}(\Omega,T) = \sum_{N=0} \exp\left[N\mu(\Omega,T)/(kT)\right] Q_N(\Omega,T) &= \sum_{N=0}^{\infty} \sum_{\substack{\{n_j\} \\ \sum n_j = N}} \exp\left[(\mu(\Omega,T)-\epsilon_j)n_j/(kT)\right] \\ &= \prod_j \left\{1+\exp\left[(\mu(\Omega,T)-\epsilon_j)/(kT)\right]\right\},\end{aligned} \tag{2.4}$$

for the case of Fermi statistics. By taking the partial derivative of $\log\mathcal{Q}$ with respect to the parameter μ, we can obtain in the usual manner,

$$N = \sum_j \frac{1}{\exp[(\epsilon_j-\mu)/kT]+1}, \tag{2.5}$$

where here $N = 1$, the average number of occupied states of the system, which fixes μ, as a function of the temperature and the volume. Since for the canonical partition function

$Q_N(\Omega, T)$, as usual we have $kT \log Q_N = -A(\Omega, T)$, where $A(\Omega, T)$ is the Helmholtz free energy, we deduce directly for (2.4) in the usual way by considering only the term in the sum corresponding to N,

$$A(\Omega, T) = N\mu(\Omega, T) - kT \sum_j \log \{1 + \exp\left[(\mu(\Omega, T) - \epsilon_j)/(kT)\right]\} \tag{2.6}$$

The energy is given from the Helmholtz free energy by the thermodynamic relation,

$$U = A - T \left.\frac{\partial A}{\partial T}\right|_\Omega = \sum_j \frac{\epsilon_j - T \left.\frac{\partial \epsilon_j}{\partial T}\right|_\Omega}{\exp[(\epsilon_j - \mu)/kT] + 1}. \tag{2.7}$$

We remark that normally, $\partial \epsilon_j / \partial T|_\Omega = 0$ and so is not included in the text book presentations. However, in our case, our treatment of the many-body effects induces a temperature dependence in energy eigenvalues in the cellular equations. It may at first sight seem surprising that although we start with a system in which the potentials in the Hamiltonian are independent of density and temperature that we could end up with this sort of dependence in the cellular equations. This sort of dependence occurs naturally when one goes beyond the independent electron approximation. As an example, consider the exchange energy which arises due to the anti-symmetry of the electron wave function. In the text book derivation [35] of this electron-electron interaction term for free electrons at zero temperature the Fermi momentum enters directly in the effective interaction term. Since the Fermi momentum is proportional to the cube root of the density, we get a direct dependence on the density in the effective interaction term. As the temperature increases, the distribution of the electron states no longer has a sharp cut-off at the Fermi surface, but is smeared out there. This difference in the energy distribution of the electrons will likewise cause a dependence of the effective interaction on the temperature as well.

The pressure is also given from the Helmholtz free energy by the thermodynamic relation

$$p = -\left.\frac{\partial A}{\partial \Omega}\right|_T = \sum_k \frac{\left.\frac{\partial \mu}{\partial \Omega}\right|_T - \left.\frac{\partial \epsilon_k}{\partial \Omega}\right|_T}{\exp[(\epsilon_k - \mu)/kT] + 1} - N \left.\frac{\partial \mu}{\partial \Omega}\right|_T,$$

$$= -\sum_k \frac{\left.\frac{\partial \epsilon_k}{\partial \Omega}\right|_T}{\exp[(\epsilon_k - \mu)/kT] + 1}. \tag{2.8}$$

It will be useful to rewrite (2.8) in terms of the "radius" r_b, or typical linear dimension of the cell as,

$$p\Omega = -\frac{1}{3}\sum_k \frac{r_b \left.\frac{\partial \epsilon_k}{\partial r_b}\right|_T}{\exp[(\epsilon_k - \mu)/kT] + 1}. \tag{2.9}$$

A remark at this point is worthwhile. It is common to see in text books the expression $p\Omega = kT \log \mathcal{Q}$. This result is only valid in the case where the Gibbs free energy $G = N\mu$, as is usually so and is certainly true for the ideal Fermi gas. In general,

$$G = A - \Omega \left.\frac{\partial A}{\partial \Omega}\right|_T = N\mu(\Omega, T) \tag{2.10}$$

$$-kT\sum_j \log\{1 + \exp[(\mu(\Omega,T) - \epsilon_j)/(kT)]\} - \frac{1}{3}\sum_k \frac{r_b \left.\frac{\partial \epsilon_k}{\partial r_b}\right|_T}{\exp[(\epsilon_k - \mu)/kT] + 1}.$$

The last two terms cancel each other for the idea gas case and correspond to the two forms of $f_{\frac{5}{2}}$ given in (3.2) given below. For reference, the entropy S can be obtained from (2.6), (2.7) and the thermodynamic relation $A = U - TS$.

Thus, in general, the computation of the pressure, *etc.*, is reduced to computations within a single cell. When we observe that for an ideal gas every eigenvalue is of the form $\hbar^2\kappa^2/(2mr_b^2)$, with κ independent of r_b, then for the ideal Fermi gas,

$$r_b \frac{\partial \epsilon_j}{\partial r_b} = -2\epsilon_j, \tag{2.11}$$

The substitution of this result into (2.9) yields the well known result,

$$p\Omega = \frac{2}{3}U. \tag{2.12}$$

The boundary conditions (2.1) and (2.2) are known to be sufficient to produce a discrete set of states for each value of $\vec{k}$. Thus in principle what one needs to do is to compute these quantities for every $\vec{k}$ in the first Brillouin zone, then to integrate over the zone and sum over the discrete states as indicated in (2.5) for various μ's, in order to determine μ as a function of r_b and the temperature T. From this determination one can then substitute it in (2.7), *et seq.* to determine the various thermodynamic quantities as predicted by our cellular model. The computation of the necessary derivatives is discussed in Appendix A.

III. CUBIC CELLULAR MODEL FOR AN IDEAL FERMI GAS

The standard formulas [34] for the ideal Fermi gas (of chargeless electrons) are,

$$\zeta = \frac{N}{2\Omega}\left(\frac{h^2}{2\pi mkT}\right)^{\frac{3}{2}} = f_{\frac{3}{2}}(z) = \frac{2}{\sqrt{\pi}}\int_0^\infty \frac{zy^{\frac{1}{2}}e^{-y}\,dy}{1+ze^{-y}}, \tag{3.1}$$

where ζ is the de Broglie density which measures the importance of quantum effects, N is the number of electrons, Ω is the volume, and m is the electron mass and $z = \exp(\mu/kT)$ in the notation of (2.5). The pressure equation is

$$\frac{p\Omega}{NkT} = \frac{f_{\frac{5}{2}}(z)}{f_{\frac{3}{2}}(z)}, \quad f_{\frac{5}{2}}(z) = \frac{2}{\sqrt{\pi}}\int_0^\infty y^{\frac{1}{2}}\log(1+ze^{-y})\,dy = \frac{4}{3\sqrt{\pi}}\int_0^\infty \frac{zy^{\frac{3}{2}}e^{-y}\,dy}{1+ze^{-y}}, \tag{3.2}$$

where the second form of $f_{\frac{5}{2}}(z)$ follows from the first through an integration by parts or *vice versa*. It is instructive to re-express these equations in cellular form. Let us choose cubes of edge a such that $a^3 = \Omega/N$ so that on average there is one electron per cell. Then the reciprocal lattice is also cubic and the edge of a primitive cell is $2\pi/a$. If we make the change of variables, $y = \hbar^2k^2/(2mkT)$ then (3.1) can be rewritten as,

$$1 = \frac{2a^3}{(2\pi)^3}\int\int\int_{-\infty}^{\infty} \frac{z\exp\left(-\frac{\hbar^2k^2}{2mkT}\right)\,d\vec{k}}{1+z\exp\left(-\frac{\hbar^2k^2}{2mkT}\right)}. \tag{3.3}$$

By dividing the range of integration according to primitive cells of the reciprocal lattice we get for (3.3),

$$1 = 2\sum_{j_1=-\infty}^{+\infty}\sum_{j_2=-\infty}^{+\infty}\sum_{j_3=-\infty}^{+\infty}\left(\frac{a}{2\pi}\right)^3\int\int\int_{-\pi/a}^{\pi/a}\frac{d\vec{k}}{1+z^{-1}\exp\left[\frac{\hbar^2}{2mkT}\left(\vec{k}+\frac{2\pi}{a}\vec{j}\right)^2\right]}, \tag{3.4}$$

where the steps in the j sums are unity. The factor of 2 is a reflection of the two spin states of the electron. The corresponding formula for the pressure is, by (3.2),

$$\frac{p\Omega}{NkT} = \frac{4}{3}\sum_{j_1=-\infty}^{+\infty}\sum_{j_2=-\infty}^{+\infty}\sum_{j_3=-\infty}^{+\infty}\left(\frac{a}{2\pi}\right)^3\int\int\int_{-\pi/a}^{\pi/a}\frac{\frac{\hbar^2}{2mkT}\left(\vec{k}+\frac{2\pi}{a}\vec{j}\right)^2\,d\vec{k}}{1+z^{-1}\exp\left[\frac{\hbar^2}{2mkT}\left(\vec{k}+\frac{2\pi}{a}\vec{j}\right)^2\right]}, \tag{3.5}$$

We are now in a position to compare these exact results for the ideal gas with the results of the cellular model described in the previous section. First, if $\vec{k} = 0$, then $\phi(\vec{r}) = \exp(i\vec{s}\cdot\vec{r})$ satisfies (2.3) with $E(0) = \hbar^2 s^2/(2m)$ and if each component of $\vec{s}$ is an integral multiple of $2\pi/a$, where a is again the cell edge, the solutions also satisfy the boundary conditions. When $\vec{k} \neq 0$ then it is easy to verify that $\phi(\vec{r}) = \exp(i\vec{s}\cdot\vec{r})$ still satisfies (2.3) and the boundary conditions with the same restrictions on $\vec{s}$. However, now $E(\vec{k}) = \hbar^2(\vec{s}+\vec{k})^2/(2m)$. When this is substituted in (2.7), (2.12) gives us exactly (3.5). Thus the cubic cell model is exact for the ideal gas. It is not difficult to persuade one's self that the same is true for any Bravias lattice cell model, as it just amounts to a reorganization of the intergals.

It is of interest to investigate what is involved in the numerical evaluation of the properties of the ideal Fermi gas by this method, as later on we will be interested in the accuracy of the spherical approximation to the cell model and in the calculation of models with Coulomb forces added. As the integrals are symmetric in the 8-octants, we can reduce the integration to a single octant. To do so, it is convenient to shift the Brillouin zone to $0 \leq k_i \leq 2\pi/a$; then we don't divide any Brillouin zones in the process. Hence (3.4) becomes,

$$1 = 16 \sum_{j_1=0}^{+\infty} \sum_{j_2=0}^{+\infty} \sum_{j_3=0}^{+\infty} \int\int\int_0^1 \frac{d\vec{\kappa}}{1+\exp\left[\pi(2\zeta)^{\frac{2}{3}}\left(\vec{\kappa}+\vec{\jmath}\right)^2 - \mu/(kT)\right]}, \tag{3.6}$$

and (3.5) becomes

$$\frac{p\Omega}{NkT} = \frac{32\pi}{3}(2\zeta)^{\frac{2}{3}} \sum_{j_1=0}^{+\infty} \sum_{j_2=0}^{+\infty} \sum_{j_3=0}^{+\infty} \int\int\int_0^1 \frac{\left(\vec{\kappa}+\vec{\jmath}\right)^2 d\vec{\kappa}}{1+\exp\left[\pi(2\zeta)^{\frac{2}{3}}\left(\vec{\kappa}+\vec{\jmath}\right)^2 - \mu/(kT)\right]}, \tag{3.7}$$

The problem here is to do the integrals over $\vec{\kappa}$ and then do the sums over $\vec{\jmath}$. Because of the exponential these sums cutoff quite rapidly once the eigenvalues exceed the free energy μ. We have used the Euler-Maclaurin sum formula, because it is quite efficient for Gaussian type integrals. Specifically, with remainder, it is,

$$\int_0^m f(x)dx =$$

$$\tfrac{1}{2}[f(0)+f(m)] + \sum_{k=1}^{m-1} f(k) - \sum_{r=1}^{n-1} \frac{B_{2r}}{(2r)!}\left[f^{(2r-1)}(m) - f^{(2r-1)}(0)\right] - f^{(2n)}(\theta_n m)\frac{B_{2n}}{(2n)!}, \tag{3.8}$$

where the B_n are the Bernoulli numbers,

$$B_2 = \frac{1}{6}, \quad B_4 = -\frac{1}{30}, \quad B_6 = \frac{1}{42}, \quad B_8 = -\frac{1}{30}, \quad B_{10} = \frac{5}{66}, \ \ldots \tag{3.9}$$

We have found that dividing the range of each rectangular component of $\vec{\kappa}$ in $\sqrt{\pi}(2\zeta)^{\frac{1}{3}} + 1$ intervals with no Bernoulli number corrections was sufficient to give a maximum deviation of 0.2% for the pressure from the representation of Baker and Johnson [36],

$$\frac{p\Omega}{NkT} = g(\zeta) \approx \left[\frac{1 + 0.61094880\zeta + 0.12660436\zeta^2 + 0.0091177644\zeta^3}{1 + 0.080618739\zeta}\right]^{\frac{1}{3}}, \tag{3.10}$$

which is accurate to 0.1%. A binary search method was used to solve (3.6) for μ. The starting value of μ used was computed from the representation given by Baker and Johnson. The left hand side was [19] reproduced to at least on part in 10^{10}. We checked over a range of $7 \times 10^{-4} \leq \zeta \leq 7 \times 10^2$. Note is taken that the Bernoulli number corrections all vanish at the boundary where a component of $\vec{\jmath}$ is zero as this is an even function in $\vec{\kappa}$, and the others cancel in pairs, except at the large cutoff in $\vec{\jmath}$ where they are negligible anyway. Thus this particular case is not a good guide in general to the expected number of Bernoulli number corrections for this accuracy.

IV. SPHERICAL CELLULAR MODEL FOR AN IDEAL FERMI GAS

As background to the spherical cellular model, let us first consider the body-centered cubic or the face-centered cubic lattice. These lattices are reciprocals of each other as is very well known. Their primitive cells are more nearly spherical that for the simple cubic lattice. For the ideal Fermi gas problem we can again choose the single electron eigenfunction to be of the form $\exp(i\vec{p} \cdot \vec{r})$ where $\vec{p}$ lies on the reciprocal lattice and couple the sum over the reciprocal lattice with an intergal over the first Brillouin zone. The same structure as explained above for the simple cubic lattice continues to work here and reproduces the ideal Fermi gas results in the same way. If for example we take $\vec{p} = n\vec{b}_1$ where $\vec{b}_1$ is one of the basic reciprocal lattice vectors, then we can write the eigenfunction in terms of the spherical basis system as

$$e^{i\vec{p}\cdot\vec{r}} = \sum_{l=0}^{\infty}(2l+1)i^l P_l\left(\cos\theta_{rp}\right)j_l\left(rp\right), \tag{4.1}$$

where the $P_l\left(x\right)$ are the Legendre polynomials and the $j_l\left(x\right)$ are the spherical Bessel functions. If we choose the length of $\vec{r}$ to be $\pi/|\vec{b}_1|$ then we can, if we wish, select equivalent boundary conditions for a sphere of that radius to be

$$e^{in\pi\cos\theta_{rp}} = \sum_{l=0}^{\infty}(2l+1)i^l P_l\left(\cos\theta_{rp}\right)j_l\left(n\pi\right), \tag{4.2}$$

on its surface, and we will have defined this eigenfunction in the sphere. It in turn can be decomposed into its even and odd parts under inversion. On the surface of this sphere they are

$$\phi_e = \cos(n\pi\cos\theta_{pr}), \quad \phi_o = i\sin(n\pi\cos\theta_{pr}). \tag{4.3}$$

In order to insure periodicity in the direction $\vec{b}_1$ we note $\phi_o = 0$ automatically here, and by differentiation, we find the $\vec{b}_1\cdot\vec{\nabla}\phi_e = 0$ here as well. In the tangent plane perpendicular to $\vec{b}_1$, we have by the usual theory of lattices, two of the basic vectors for the lattice. In this whole plane, the same two boundary conditions $\phi_o = 0$, $\vec{b}_1\cdot\phi_e = 0$ hold as mentioned above for the poles of the sphere. This set of boundary conditions reflects the usual three-dimensional periodicity of a space lattice. In other directions we see the oscillating boundary conditions describe by (4.2-3) above, which of course reflect the existence of special directions for the space lattice.

These boundary conditions would be rather hard to use in the spherical coordinate framework if we didn't already know the result, as they mix a potentially large number of different l states and greatly increase the solution effort. For the ideal gas cases, of course, there is no problem as we have the solution already, but a problem would arise if we were to try to add a spherically symmetric potential. Besides this sort of boundary conditions violates the spirit of the spherical cellular model as it has preferred directions. The spherical cellular model is necessarily an approximation as one can not fill space with spheres of constant diameter and the whole Bravias lattice structure which works so neatly for actual space lattices is inapplicable for spherical cells.

Alternatively we can start with equation (2.3) and impose the boundary conditions (2.1)-(2.2) for periodicity in all directions at every point on the surface of the spherical cell of radius r_b. These requirements lead to the conditions,

$$\vec{n} \cdot \vec{\nabla} \phi_{\text{even}} = 0, \quad \phi_{\text{odd}} = 0 \tag{4.4}$$

on the surface of the spherical cell. The first Brillouin zone is taken to be $|\vec{k}| \leq k_B = (9\pi/2)^{1/3}/r_b$. In the case $\vec{k} = \vec{0}$, we can construct a basis set of solutions of (2.3) in the spherical cell with these boundary conditions. They imply, in short that the radial derivative of the part which is even under inversion must vanish at the surface and the value of the odd part must vanish on the surface of the cell. Specifically, the basis set is

$$|l, m, \lambda\rangle = Y_{lm}(\theta, \phi) N_{l\lambda} j_l(p_{l\lambda} r), \quad m = -l, -l+1, \ldots, l, \quad l = 0, 1, \ldots, \quad \lambda = 1, 2, \ldots, \tag{4.5}$$

where $Y_{l,m}(\theta, \phi)$ are the usual normalized spherical harmonics, and are, in terms of the associated Legendre Polynomials, $P_l^m(\cos\theta)$

$$Y_{l,m}(\theta, \phi) = \left(\frac{(2l+1)(l-|m|)!}{4\pi(l+|m|)!} \right)^{1/2} P_l^{|m|}(\cos\theta) e^{im\phi}. \tag{4.6}$$

The quantities $p_{l,\lambda}$ are determined by the boundary conditions through the requirements,

$$\begin{aligned} j_l(p_{l,\lambda} r_b) &= 0, \quad l \text{ odd}, \\ j_l'(p_{l,\lambda} r_b) &= 0, \quad l \text{ even}. \end{aligned} \tag{4.7}$$

Finally the $N_{l,\lambda}$ are given by

$$1 = N_{l,\lambda}^2 \int_0^{r_b} j_l^2(p_{l,\lambda} r) r^2 \, dr = \tfrac{1}{2} r_b^3 \left[j_l^2(p_{l,\lambda} r_b) - j_{l-1}(p_{l,\lambda} r_b) j_{l+1}(p_{l,\lambda} r_b) \right] N_{l,\lambda}^2, \tag{4.8}$$

where we take $j_{-1}(x) = -n_0(x) = \cos x / x$. This set of basis functions is a complete orthonormal set. It is not the only possible such set, but it is appropriate to our present needs.

The next step is to resolve the operator $H' = -(i\hbar^2/m)\vec{k} \cdot \vec{\nabla}$ in this basis. Since the spherical cell has no preferred direction, we have, for convenience, taken $\vec{k}$ to be parallel to the z-axis. It is to be noticed that the various m states are not mixed by this operator

because it commutes with the z-component of angular momentum. This resolution requires some straightforward, but tedious computation.

$$H'|l,m,\lambda\rangle = \frac{-i\hbar^2 k}{m}\left[\frac{2l+1}{4\pi}\frac{(l-|m|)!}{(l+|m|)!}\right]^{\frac{1}{2}} e^{im\phi}\Big[\frac{l-m+1}{2l+1}P^m_{l+1}(x)\left(p_{l,\lambda}j_l'(p_{l,\lambda}r) - \frac{l}{r}j_l(p_{l,\lambda}r)\right)$$
$$+\frac{l+m}{2l+1}P^m_{l-1}(x)\left(p_{l,\lambda}j_l'(p_{l,\lambda}r) + \frac{l+1}{r}j_l(p_{l,\lambda}r)\right)\Big]N_{l,\lambda}, \tag{4.9}$$

Thus, the results are $\langle l',m',\lambda'|H'|l,m,\lambda\rangle = 0$ unless $|l'-l| = 1$. The non-zero elements are

$$\langle l-1,m',\lambda'|H'|l,m,\lambda\rangle =$$
$$\begin{cases} \frac{-i\hbar^2 k p_{l,\lambda}}{m}\left(\frac{l^2-m^2}{4l^2-1}\right)^{\frac{1}{2}}\delta_{m',m}\left[\frac{2p_{l,\lambda}j_{l-1}'(p_{l,\lambda}r_b)}{r_b(p^2_{l,\lambda}-p^2_{l-1,\lambda'})|j_{l-1}(p_{l,\lambda}r_b)|}\left(\frac{j_{l-1}(p_{l-1,\lambda'}r_b)}{-j_{l-1}''(p_{l-1,\lambda'}r_b)}\right)^{\frac{1}{2}}\right], & \text{for } l \text{ odd} \\ \frac{-i\hbar^2 k p_{l,\lambda}}{m}\left(\frac{l^2-m^2}{4l^2-1}\right)^{\frac{1}{2}}\delta_{m',m}\left[\frac{2p_{l-1,\lambda'}j_{l-1}(p_{l,\lambda}r_b)}{r_b(p^2_{l,\lambda}-p^2_{l-1,\lambda'})(-j_l(p_{l,\lambda}r_b)j_l''(p_{l,\lambda}r_b))^{\frac{1}{2}}}\right], & \text{for } l \text{ even} \end{cases} \tag{4.10}$$

and

$$\langle l+1,m',\lambda'|H'|l,m,\lambda\rangle =$$
$$\begin{cases} \frac{-i\hbar^2 k p_{l,\lambda}}{m}\left(\frac{(l+1)^2-m^2}{4(l+1)^2-1}\right)^{\frac{1}{2}}\delta_{m',m}\left[\frac{2p_{l,\lambda}j_{l+1}'(p_{l,\lambda}r_b)}{r_b(p^2_{l,\lambda}-p^2_{l+1,\lambda'})|j_{l+1}(p_{l,\lambda}r_b)|}\left(\frac{j_{l+1}(p_{l+1,\lambda'})}{-j_{l+1}''(p_{l+1,\lambda'}r_b)}\right)^{\frac{1}{2}}\right], & \text{for } l \text{ odd} \\ \frac{-i\hbar^2 k p_{l,\lambda}}{m}\left(\frac{(l+1)^2-m^2}{4(l+1)^2-1}\right)^{\frac{1}{2}}\delta_{m',m}\left[\frac{-2p_{l+1,\lambda'}j_{l+1}(p_{l,\lambda}r_b)}{r_b(p^2_{l,\lambda}-p^2_{l+1,\lambda'})(-j_l(p_{l,\lambda}r_b)j_l''(p_{l,\lambda}r_b))^{\frac{1}{2}}}\right], & \text{for } l \text{ even} \end{cases} \tag{4.11}$$

As the operator H' is Hermitian, but doesn't look so in this mode of expression, we remark that its Hermiticity can be explicitly verified by use of the Bessel function identities,

$$p_{l,\lambda}j_{l+1}(p_{l+1,\lambda'}r_b)j_{l+1}'(p_{l,\lambda}r_b) = p_{l+1,\lambda'}j_{l+1}(p_{l,\lambda}r_b)j_l(p_{l+1,\lambda'}r_b), \quad l \text{ odd},$$
$$p_{l+1,\lambda'}j_l(p_{l,\lambda}r_b)j_l'(p_{l+1,\lambda'}r_b) = p_{l,\lambda}j_{l+1}(p_{l,\lambda}r_b)j_l(p_{l+1,\lambda'}r_b), \quad l \text{ even}, \tag{4.12}$$

where use has been made of the standard Bessel function identities and also in particular, the boundary conditions (4.7). It is to be noticed that $j_l''(p_{l,\lambda}r_b)$ only appears in (4.10) and (4.11) for even l. In this case, as $j_l'(p_{l,\lambda}r_b) = 0$, the j'' terms can be replaced, using the spherical Bessel function equation,

$$j_l''(p_{l,\lambda}r_b) = -\left(1 - \frac{l(l+1)}{p^2_{l,\lambda}r_b^2}\right)j_l(p_{l,\lambda}r_b), \tag{4.13}$$

which eases the problem of the evaluation of the expressions.

In the case where $p_{l\pm1,\lambda'} = p_{l,\lambda}$ the [] terms in (4.10) and (4.11) considerable simplify. They are

$$\left[\ \right] \to -\left(1 - \frac{L(L+1)}{p_{l,\lambda}^2 r_b^2}\right)^{\frac{1}{2}}, \tag{4.14}$$

where for l even, $L = l$ and for l odd, $L = l-1$ for (4.10) and $L = l+1$ for (4.11) respectively.

One might think that the occurrence of degeneracy, other than between the states with different z-components of angular momentum, which do not mix in this case, would be accidental and rare. However, degeneracy and near degeneracy, is quite common in this basis. First, since $j_0'(z) = -j_1(z)$, the $m = 0$ component of the $l = 1$ member of our basis states is always exactly degenerate with the corresponding $l = 0$ state. In general, for the higher order zeros, we have the asymptotic expansions [37]. The $s\underline{\text{th}}$ zero of $j_l'(z)$ is

$$\hat{z}_s(l) = \beta - \frac{(2l+1)^2 + 7}{8\beta} + O(\beta^{-3}), \quad \beta = \pi(s + \tfrac{1}{2}l - \tfrac{1}{2}), \tag{4.15}$$

and the $s\underline{\text{th}}$ zero of $j_l(z)$ is

$$z_s(l) = \beta - \frac{(2l+1)^2 - 1}{8\beta} + O(\beta^{-3}), \quad \beta = \pi(s + \tfrac{1}{2}l). \tag{4.16}$$

By way of comparison we consider the results from (4.15) for $l = 2\mu + 1$ and from (4.16) for $l = 2\mu$. In this case $\beta = \pi(s + \mu)$ for both cases so to leading order they are degenerate. Taking the difference we get

$$z_s(2\mu) - \hat{z}_s(2\mu + 1) = 2\left(\frac{\mu + 1}{\beta}\right) + O(\beta^{-3}), \tag{4.17}$$

So for large s we get very near degeneracy. For smaller values of s, except for the $l = 0, 1$ correspondence, the degeneracy is not too bad but not so close. We report some of the values in Table I [38].

If there is a near degeneracy so that for some λ'' and λ', $p_{l,\lambda''} \approx p_{l\pm1,\lambda'}$ then, without the compensating vanishing or near vanishing of $p_{l,\lambda''}^2 - p_{l\pm1,\lambda'}^2$ the vanishing, or near vanishing of the numerators in (4.10) or (4.11) causes the corresponding matrix element of H' to vanish or nearly vanish. With this observation as guidance, we will now divide the Hamiltonian matrix into blocks characterized by a value of m, the z-component of the angular momentum, and all those states which are degenerate in leading order as expressed in (4.14) and (4.15). The

largest block will be for the $m = 0$ case and the lowest energy state of the largest value of l retained.

It is to be noticed that the matrix elements of H' depend on m. This dependence adds greatly to the length and complexity of the computation. For numerical expediency, within each block of degenerate, or nearly degenerate states, we replace the resulting eigenvalues with the eigenvalue plus or minus the root mean square deviation over its block of the eigenvalues due to H'. These latter values are easily computed by taking the trace of $(H_0 + H')^2$ for that block. The exception is for the lowest $l = 0$ state which is not degenerate nor nearly degenerate with any other state, and so no change is made here on account of H'. This treatment agrees with that of Bardeen [39] for the ground state case.

The necessary partial traces to be taken are those of $(H')^2$. One convenient way to get them is to start from the result (4.9), and use the completeness formula, $\langle l, m, \lambda | (H')^2 | l, m, \lambda \rangle = \sum_{l', m', \lambda'} \langle l, m, \lambda | H' | l', m', \lambda' \rangle \langle l', m', \lambda' | H' | l, m, \lambda \rangle$. These results, together with the completeness of the $\phi_{l \pm 1, \lambda}(r)$ over all λ for $0 \leq r \leq r_b$ allow us to deduce, by direct computation, the conclusion,

$$\langle l, m, \lambda | (H')^2 | l, m, \lambda \rangle = 4 \left(\frac{\hbar^2 k^2}{2m} \right) \left(\frac{2l^2 + 2l - 1 - 2m^2}{(2l-1)(2l+3)} T_{l,\lambda} + \frac{l(l+1) - 3m^2}{(2l-1)(2l+3)} S_{l,\lambda} \right), \quad (4.18)$$

where

$$T_{l,\lambda} = -\frac{\hbar^2}{2m} \langle l, m, \lambda | \nabla^2 | l, m, \lambda \rangle, \quad S_{l,\lambda} = \frac{\hbar^2}{2m} r_b |\phi_{l,\lambda}(r_b)|^2, \quad (4.19)$$

and use was made of our boundary conditions, which imply that $\phi_{l,\lambda}(r_b)\phi'_{l,\lambda}(r_b) = 0$ for all values of l. Note that $S_{l,\lambda} = 0$ for l odd. The sum of the absolute squares over the $2l + 1$ states of the m is, by direct computation from (4.18)

$$\sum_{m=-l}^{l} \langle l, m, \lambda | (H')^2 | l, m, \lambda \rangle = 4 \left(\frac{\hbar^2 k^2}{2m} \right) \left(\frac{2l+1}{3} \right) T_{l,\lambda}, \quad (4.20)$$

where the sum over m of the $S_{l,\lambda}$ term vanishes here. The $(2l + 1)/3$ factor has the interpretation that it is the total number of states, divided by the number of spatial dimensions, as only one direction is singled out by $\vec{k}$. The result in (4.20) corresponds to averaging over

all the directions of $\vec{k}$ as the sum over the m-states is independent of the original direction chosen for $\vec{k}$, and so is in line with the concept of the spherical cell.

The next step is to sum over the l values of the degenerate or nearly degenerate block. For the ωth excited state of $l = 0$ this sum would be up to L which is the lesser of the maximum l value considered or 2ω. Thus the root mean square value, $\Delta_\omega(k)$ for this block would be given in units of the Brillouin energy by,

$$\left[\frac{\hbar^2 k_B^2}{2m}\Delta_\omega(k)\right]^2 = \frac{4}{(L+1)^2}\left(\frac{\hbar^2 k^2}{2m}\right)\sum_{l=0}^{L-1}\left(\frac{2l+1}{3}\right)T_{l,\omega-[(l+1)/2]}. \tag{4.21}$$

In a manner similar to (3.6) and (3.7) we obtain the expressions which determine the parameter μ and the pressure. The parameter μ is given by the solution of

$$1 = 3\sum_{l=0}^{\infty}(2l+1)\sum_{n=0}^{\infty}\int_0^1 d\kappa\,\kappa^2\left\{\frac{1}{1+\exp\left((1.5\sqrt{\pi}\zeta)^{\frac{2}{3}}(e_{l,n}+\kappa^2+\kappa\Delta_{n+[(l+1)/2]})-\mu/kT\right)}\right.$$
$$\left.+\frac{1}{1+\exp\left((1.5\sqrt{\pi}\zeta)^{\frac{2}{3}}(e_{l,n}+\kappa^2-\kappa\Delta_{n+[(l+1)/2]})-\mu/kT\right)}\right\}, \tag{4.22}$$

where we use the notation $e_{l,n} = p_{l,n}^2/k_B^2$ and where $3 = 2\times 3\times\frac{1}{2}$ and the 2 is for the two electron states, the 3 normalizes the intergal, and the $\frac{1}{2}$ compensates for the two $\pm\Delta$ terms. For the pressure, remembering the factor of $\frac{2}{3}$ given by (2.12), we get,

$$\frac{p\Omega}{NkT} = 2(1.5\sqrt{\pi}\zeta)^{\frac{2}{3}}\sum_{l=0}^{\infty}(2l+1)\sum_{n=0}^{\infty}\int_0^1 d\kappa\,\kappa^2\times$$
$$\left\{\frac{e_{l,n}+\kappa^2+\kappa\Delta_{n+[(l+1)/2]}(k_B)}{1+\exp\left((1.5\sqrt{\pi}\zeta)^{\frac{2}{3}}(e_{l,n}+\kappa^2+\kappa\Delta_{n+[(l+1)/2]})-\mu/kT\right)}\right.$$
$$\left.+\frac{e_{l,n}+\kappa^2-\kappa\Delta_{n+[(l+1)/2]}(k_B)}{1+\exp\left((1.5\sqrt{\pi}\zeta)^{\frac{2}{3}}(e_{l,n}+\kappa^2-\kappa\Delta_{n+[(l+1)/2]})-\mu/kT\right)}\right\}. \tag{4.23}$$

This form is analogous to the second form for $f_{\frac{5}{2}}$ in (3.2).

A form analogous to the first form for $f_{\frac{5}{2}}$ in (3.2) is

$$\frac{p\Omega}{NkT} =$$
$$3\sum_{l=0}^{\infty}(2l+1)\sum_{n=0}^{\infty}\int_0^1 d\kappa\,\kappa^2\left\{\log\left[1+\exp\left(\mu/kT-(1.5\sqrt{\pi}\zeta)^{\frac{2}{3}}(e_{l,n}+\kappa^2+\kappa\Delta_{l,n})\right)\right]\right.$$
$$\left.+\log\left[1+\exp\left(\mu/kT-(1.5\sqrt{\pi}\zeta)^{\frac{2}{3}}(e_{l,n}+\kappa^2-\kappa\Delta_{l,n})\right)\right]\right\}, \tag{4.24}$$

It is to be noted that the structure of (4.24) is such that the pressure is necessarily positive. We can obtain an expression which makes the integrals and the numerical approximations used to evaluate them parallel to those of (4.22) and (4.23), if we integrate (4.24) by parts with respect to κ. The result is

$$\frac{p\Omega}{NkT} =$$
$$\sum_{l=0}^{\infty}(2l+1)\sum_{n=0}^{\infty}\Big\{\log\Big[1+\exp\Big(\mu/kT-(1.5\sqrt{\pi}\zeta)^{\frac{2}{3}}(e_{l,n}+1+\Delta_{n+[(l+1)/2]})\Big)\Big]$$
$$+\log\Big[1+\exp\Big(\mu/kT-(1.5\sqrt{\pi}\zeta)^{\frac{2}{3}}(e_{l,n}+1-\Delta_{n+[(l+1)/2]})\Big)\Big]\Big\}$$
$$+(1.5\sqrt{\pi}\zeta)^{\frac{2}{3}}\sum_{l=0}^{\infty}(2l+1)\sum_{n=0}^{\infty}\int_0^1 d\kappa\,\kappa^2\times$$
$$\Big\{\frac{2\kappa^2+\kappa\Delta_{n+[(l+1)/2]}(k_B)}{1+\exp\Big((1.5\sqrt{\pi}\zeta)^{\frac{2}{3}}(e_{l,n}+\kappa^2+\kappa\Delta_{n+[(l+1)/2]})-\mu/kT\Big)}$$
$$+\frac{2\kappa^2-\kappa\Delta_{n+[(l+1)/2]}(k_B)}{1+\exp\Big((1.5\sqrt{\pi}\zeta)^{\frac{2}{3}}(e_{l,n}+\kappa^2-\kappa\Delta_{n+[(l+1)/2]})-\mu/kT\Big)}\Big\}. \tag{4.25}$$

In order to compute the thermodynamics of the ideal gas for a spherical cellular model we first compute the eigenvalues and eigenvectors of the above mentioned blocks. These block matrices are tridiagonal and so the numerical computations are straightforward and quick. The eigenvalue spectrum allows us to compute by (4.22) the value of the parameter μ, and then in turn by (4.23) or (4.25) the value of the pressure. Remember that as discussed in the Sec. II, we need to pick out a discrete set of $\vec{k}$'s and appropriately sum over them to simulate the integral over the first Brillouin zone. We have evaluated these equations numerically and solve for μ as described in the section on the cubic cellular model. We find that the results of our spherical approximation for the pressure using (4.25) is accurate to within -2.2 to $+1.2$ percent, and using (4.23) is accurate to within about -2.5 to $+4.9$ percent. Form (4.25) is somewhat more accurate in the ideal gas case, however the form (4.23) must be used in later sections as (4.25) does not hold in general. We illustrate these results in Fig. 1. Our results for z are accurate -10 to $+4$ percent. However, the equations for z are not very sensitive to the value of z. That is to say, the change in the left hand side of (4.22) is proportionately much less than the change in z. It is to be noticed that for

(4.25) in Fig. 1 the smallest three plus decades (high temperature) and about the first two decades (low temperature) in ζ are accurate to fractions of a percent, and tending rapidly to the correct values in each limiting case. For form (4.23) it is to be noticed that in Fig. 1 the smallest two decades (high temperature) and about the first decade (low temperature) in ζ are accurate to fractions of a percent, and also tend rapidly to the correct values in each limiting case. We have studied the same range of ζ here as we did in the case of the cubic cellular model in the previous section.

The technical details of the calculations are as follows. We have divided the range of r up into the larger of $16x$ or $2x\sqrt{T_{\text{maximum}}}$, where T_{maximum} is in electron volts, and x looks ahead to the next section and is defined as

$$x = \left(\frac{128}{9\pi^2}\right)^{\frac{1}{3}} \frac{me^2 r_b}{\hbar^2}, \tag{4.26}$$

where e is the charge on the electron. The number of partial waves taken is governed by

$$L \geq \frac{1}{2}(\sqrt{1+3.54x} - 1) + 10, \tag{4.27}$$

which also looks ahead to the next section and keeps the minimum value of the potential plus the angular momentum barrier for the maximum value of l outside the considered sphere. The 10 is added for safety. In addition we require that

$$L \geq \left\{x + x^2 T_{\text{maximum}} \left[0.86466 + \max\left(0, \ln(x^2 T_{\text{maximum}})/17.3479\right)\right]\right\}^{\frac{1}{2}}, \tag{4.28}$$

which enforces the condition that the minimum acceptable value of the potential plus the angular momentum barrier at the surface of the sphere should be $15 + 2\ln(L+1)$. The L dependent part is to take account of the fact that there are about $(L+1)^2$ degenerate, or nearly degenerate states contributing at that energy level. This restriction leads to a reduction in the relative term size of the order of 10^6. In the case reported in Fig. 1, $L = 213$ and the number of intervals in r is 353. The method of integration over κ discussed in the previous section is used here with two Euler-Maclaurin corrections. We selected $16(1.5\sqrt{\pi}\zeta)^{\frac{1}{3}} + 10$ intervals for the κ integration, which refines the rule in the previous

section by an order of magnitude because the Euler-Maclaurin corrections do not cancel out as they did for the cubic model. We have checked that these rules are adequate for our purposes by running test cases where they numbers were at least double, and found that the resultant changes were not at a significant level.

V. SPHERICAL CELLULAR MODEL FOR AN ION-ELECTRON GAS

The addition of Coulomb forces to the spherical model of an ideal Fermi gas is not straight forward, if we wish to be able to compute numerical results from our model. We will in the main use the independent electron model with some modifications where required. Initially we will begin with a discussion of hydrogen ($Z = 1$), which is conceptually somewhat simpler. In the highly dilute, cold limit, following Wigner and Seitz [33], we start with the Heitler-London atomic approximation, together with the boundary conditions as discussed in section II, and so we start with the equation,

$$\frac{\hbar^2 k^2}{2m}\phi_\lambda(\vec{r}) - \frac{i\hbar^2}{m}\vec{k}\cdot\vec{\nabla}\phi_\lambda(\vec{r}) - \frac{\hbar^2}{2m}\nabla^2\phi_\lambda(\vec{r}) - \frac{e^2}{r}\phi_\lambda(\vec{r}) = E_\lambda(\vec{k})\phi_\lambda(\vec{r}). \tag{5.1}$$

As is well known, the boundary condition $\phi'(r_b) = 0$ for the ground state (even parity) leads to a lower energy than that for the atomic ground state [30]. This boundary condition "pushes" the electrons which would have been outside the cell into the cell and has the effect of concentrating them in the outer part of the cell (relative to the atomic wave function). This can be viewed as clustering electrons between the two adjacent ions, and thus lowering the energy and forming a bond between them. This effect, in some sense, represents the polarization attraction of two atoms, but is, of course, sphericalized in our model.

In our subsequent discussions it will be useful to introduce the relative strength of the Coulomb energy to the thermal energy by

$$y^2 = \frac{e^2}{r_b kT}. \tag{5.2}$$

The ideal Fermi gas of the previous section is characterized by $y = 0$, and the cold isolated atom picture of the previous paragraph by large y. The properties of the ideal gas depend on

ζ alone, (3.1). A considerable amount is known about the small y behavior from many-body perturbation theory. In particular, it is known that the sum [40] of the ion-ion repulsion, electron-electron repulsion and the ion-electron direct terms cancel in first order in e^2 for electrically neutral systems. The only term which contributes to this order is the so-called exchange term. Let us now examine the properties of the cellular model in this regime. The ion-ion repulsion term is not in evidence because there is only one ion in the cell and the ion-ion term for ions outside the cell is cancelled by the ion-electron attraction terms with the electrons outside the cell. We do have the ion-electron attraction term within the cell. As in this regime the electron density is uniform in the cell, we can easily compute this energy as

$$E_{\mathrm{i-e}} = -\frac{3}{4\pi r_b^3}\int_{|\vec{r}|\leq r_b} d\vec{r}\,\frac{e^2}{r} = -\frac{3e^2}{2r_b}. \tag{5.3}$$

This derivation would normally be supposed to be valid only for high temperature (small ζ), but for our boundary conditions the ground state wave function for the ideal gas is just a constant. This circumstance leads to a uniform electron density for very low temperature (large ζ). In Fig. 2 we plot this energy divided by the result in (5.3). We have calculated this quantity using the spherical cellular model of the ideal gas as described in Sec. IV. It is to be observed that the quantity is substantially independent of ζ. There is about a 6 percent dip near $\zeta = 1$, but this may reflect an inadequacy of our spherical cellular model.

In addition there are the electron-electron and ion-ion repulsion energies. These arise because we are really treating an system of N electrons and N ions, each of which is present in a particular cell with probability $1/N$. This energy can be computed directly as is done in the "Hartree term" [35]. As usual, even though there is no self-interaction, the weighted square of the wave function need not be subtracted as it only contributes of the order of $1/N$ to the results. Thus we get,

$$\begin{aligned} E_{\mathrm{e-e}} &= \left(\frac{3}{4\pi r_b^3}\right)^2 \int_{|\vec{r}_1|\leq r_b} d\vec{r}_1 \int_{|\vec{r}_2|\leq r_b} d\vec{r}_2\,\frac{e^2}{|\vec{r}_1-\vec{r}_2|} \\ &= \frac{3e^2}{2r_b}\left(\frac{3}{4\pi r_b^3}\right)\int_{|\vec{r}_1|\leq r_b} d\vec{r}_1\left[1-\frac{1}{3}\left(\frac{r_1}{r_b}\right)^2\right] = \frac{6e^2}{5r_b}, \end{aligned} \tag{5.4}$$

$$E_{\mathrm{i-i}}=\left(\frac{3}{4\pi r_b^3}\right)^2\int_{|\vec{r}_1|\le r_b}d\vec{r}_1\int_{|\vec{r}_2|\le r_b}d\vec{r}_2\,\frac{e^2}{|\vec{r}_1-\vec{r}_2|}=\frac{6e^2}{5r_b}.$$

It is to be noticed that $E_{\mathrm{i-e}}+0.5(E_{\mathrm{e-e}}+E_{\mathrm{i-i}})$ does not cancel. The physical reason for this is that in this regime the ions are also uniformly distributed, there by reducing the ion-electron attraction so exact cancellation occurs. However, since we are not going to adjust the $-e^2/r$ term in the Hamiltonian because of its correctness for large y, we will instead add $E_{\mathrm{i}}=3e^2/(10r_b)$ to $E_{\mathrm{i-e}}$ to compensate for the ion distribution effect. The addition of constant amounts to all the energy levels, by (2.5), adds the same constant to μ. The changes in the potential in (5.1) necessary to take account of of all the direct terms of the first order in y^2 are the addition of the two terms,

$$E_{\mathrm{i}}=\frac{3e^2}{10r_b},\quad\text{and}\quad\tilde{V}(r)=\left(\frac{3e^2}{2r_b}-\frac{e^2r^2}{2r_b^3}\right)_{\mathrm{e-e}}+\left(\frac{6e^2}{5r_b}\right)_{\mathrm{i-i}}=\frac{27e^2}{10r_b}-\frac{e^2r^2}{2r_b^3}. \tag{5.5}$$

Because this potential is caused by interaction with the other electrons and between the ion-ion pairs, as usual, we use $\epsilon_\lambda=E_\lambda-\frac{1}{2}\langle\tilde{V}\rangle$ for the energies ϵ of Section 2. When the potential of (5.5) is averaged over the spherical cell it gives $12e^2/(5r_b)$. The net contribution is just one-half of that so we find that this term exactly cancels $E_{\mathrm{i-e}}+E_{\mathrm{i}}$ to leading order in y^2.

Note is taken that the total potential $\tilde{V}(r)-e^2/r$ serendipitiously has zero radial derivative at the surface of the cell! We will see below however that this feature is only valid to the leading order in y^2.

The "exchange term" comes from the interchange of electrons between two different states as a result of their mutual interaction via the electron-electron force. The ion-ion exchange term will be neglected here. The first order interaction energy for all values of ζ is given by Baker and Johnson [19] as,

$$E_{\mathrm{exch}}=-\frac{4\pi e^2}{(2\pi)^6}\left(\frac{4\pi r_b^3}{3}\right)\int\frac{d\vec{k}_1\,d\vec{k}_2}{(\vec{k}_1-\vec{k}_2)^2}n(\vec{k}_1)n(\vec{k}_2), \tag{5.6}$$

where $n(\vec{p})$ is the Fermi distribution function,

$$n(\vec{p})=\frac{1}{\exp\{[(\hbar^2p^2/2m)-\mu]/kT\}+1}. \tag{5.7}$$

This equation reduces to the text book result for the exchange energy when the limit $T \to 0$ is taken, where $n(\vec{p}) = 1$ for $|\vec{p}| \leq k_F$ and zero otherwise. Baker and Johnson [36] further give a representation which is good to about 0.1%. It is,

$$E_{\text{exch}} = -\frac{e^2}{2\pi r_b}\left(\frac{3}{\pi}\right)^{\frac{1}{3}} \zeta^{-\frac{4}{3}} X(\zeta), \tag{5.8}$$

where,

$$X(\zeta) \approx \frac{\pi}{2}\zeta^2 \left[\frac{1 + 0.088412769\zeta}{1 + 0.79551953\zeta + 0.19350034\zeta^2 + 0.013716390\zeta^3}\right]^{\frac{1}{3}}. \tag{5.9}$$

Clearly, this exchange term is not independent of ζ. When ζ is large, then the text book value of the exchange energy, as a function of wave number $\vec{p}$ is just given [35] by

$$\hat{V}(\vec{k}_1) = -\frac{2e^2}{\pi}k_B\left(\frac{1}{2} + \frac{k_B^2 - k_1^2}{4k_1k_B}\log\left|\frac{k_B + k_1}{k_B - k_1}\right|\right) = -\frac{2e^2}{\pi}k_B\left[1 - \frac{1}{3}\left(\frac{k_1}{k_B}\right)^2 + \ldots\right. \tag{5.10}$$

which increases from a minimum at $k_1 = 0$ in a manner proportional to k_1^2. We can also compute the results for ζ small. Here we get, by taking a factor of two times the functional derivative of (5.6) with respect to $\delta n(\vec{k}_1)$,

$$\hat{V}(\vec{k}_1) = \frac{-8\pi e^2}{(2\pi)^3}\int \frac{d\vec{k}_2}{(\vec{k}_1 - \vec{k}_2)^2} n(\vec{k}_2) \approx \frac{-8\pi e^2}{(2\pi)^3}\zeta \int \frac{d\vec{k}_2}{(\vec{k}_1 - \vec{k}_2)^2}\exp\left(-\frac{\hbar^2 k_2^2}{2mkT}\right). \tag{5.11}$$

Substituting $\vec{k}_2 = \vec{k}_3 + \vec{k}_1$ and integrating over the angles of $\vec{k}_3$, we get,

$$\begin{aligned}\hat{V}(\vec{k}_1) \approx & -\frac{2e^2\zeta}{\pi k_1}\left(\frac{2mkT}{\hbar^2}\right)\exp\left(-\frac{\hbar^2 k_1^2}{2mkT}\right)\int_0^\infty dk_3 \exp\left(-\frac{\hbar^2 k_3^2}{2mkT}\right)\sinh\left(\frac{\hbar^2 k_1 k_3}{mkT}\right)/k_3 \\ & = -\frac{2e^2\zeta}{\sqrt{\pi}}\left(\frac{2mkT}{\hbar^2}\right)^{\frac{1}{2}}\exp\left(-\frac{\hbar^2 k_1^2}{2mkT}\right) {}_1F_1\left(\frac{1}{2};\frac{3}{2};\frac{\hbar^2 k_1^2}{2mkT}\right),\end{aligned} \tag{5.12}$$

where ${}_1F_1(\frac{1}{2};\frac{3}{2};z)$ is a confluent hypergeometric function. For large k_1^2, $\hat{V}(\vec{k}_1)$ goes asymptotically to zero like k_1^{-2} and for small k_1^2 it is

$$\hat{V}(\vec{k}_1) = -\frac{2e^2}{r_b}\left(\frac{3}{\pi}\right)^{\frac{1}{3}}\zeta^{\frac{2}{3}}\left[1 - \frac{\hbar^2 k_1^2}{3mkT} + \ldots\right. \tag{5.13}$$

The usual procedure for the exchange energy is to replace its effects by an effective mass. This idea corresponds well with the small k behavior and the general shape of the exchange

energy versus the wave number, at least where there is significant statistical weight attached to the state. To implement this idea we will represent the exchange potential by

$$\hat{v}(\vec{k}_1) = \hat{V}(0) + y^2 A(\zeta)\frac{\hbar^2 k_1^2}{2m}. \tag{5.14}$$

First we may observe that the value of the exchange energy for $k_1 = 0$ is given from (5.11) by

$$\hat{V}(0) = -\frac{8\pi e^2}{(2\pi)^3}\int \frac{d\vec{k}_2}{k_2^2} n(\vec{k}_2) = -\frac{2e^2}{r_b}\zeta^{-\frac{1}{3}}\left(\frac{3}{\pi}\right)^{\frac{1}{3}}\frac{1}{\sqrt{\pi}}\int_0^\infty \frac{zy^{-\frac{1}{2}}e^{-y}\,dy}{1+ze^{-y}} = -\frac{2e^2}{r_b}\zeta^{-\frac{1}{3}}\left(\frac{3}{\pi}\right)^{\frac{1}{3}} f_{\frac{1}{2}}(z), \tag{5.15}$$

in line with the notation of (3.1). Baker and Johnson [36] have provided a representation of $f_{\frac{1}{2}}(z)$ as a function of ζ which is uniformly accurate to within 0.1%. It is

$$f_{\frac{1}{2}}(z) = \frac{1}{2}\zeta\left(\frac{v_3(\zeta)}{u_5(\zeta)}\right)^{\frac{1}{3}}, \tag{5.16}$$

where

$$v_3(\zeta) = 1 + 0.17549205\zeta + 1.1833437\times 10^{-2}\zeta^2 + 3.0923597\times 10^{-4}\zeta^3, \tag{5.17}$$

and

$$u_5(\zeta) = 1 + 1.2361522\zeta + 0.54327035\zeta^2 + 9.7985998\times 10^{-2}\zeta^3 + 6.1912639\times 10^{-3}\zeta^4 + 1.6191557\times 10^{-4}\zeta^5. \tag{5.18}$$

To determine the value of the coefficient of k_1^2 and thus the effective mass as a function of ζ, we require that the proper value of E_{exch} be reproduced. The multiplication of (5.14) by $n(\vec{k}_1)$ and the integration over $\vec{k}_1$ leads, by two times (5.8), (5.14) and (5.15) to the equation

$$-\frac{e^2}{\pi r_b}\left(\frac{3}{\pi}\right)^{\frac{1}{3}}\zeta^{-\frac{4}{3}}X(\zeta) = -\frac{2e^2}{r_b}\zeta^{-\frac{1}{3}}\left(\frac{3}{\pi}\right)^{\frac{1}{3}} f_{\frac{1}{2}}(z) + \frac{3}{2}kT\zeta^{-1}y^2 A(\zeta) f_{\frac{5}{2}}(z), \tag{5.19}$$

which determines $A(\zeta)$ to be

$$A(\zeta) = \frac{2}{3}\zeta^{\frac{2}{3}}\left(\frac{3}{\pi}\right)^{\frac{1}{3}}\left\{\frac{2f_{\frac{1}{2}}(z) - X(\zeta)/(\pi\zeta)}{f_{\frac{5}{2}}(z)}\right\}. \tag{5.20}$$

The function $f_{\frac{5}{2}}$ is just $\zeta g(\zeta)$ of (3.10). The behavior of $A(\zeta)$ when $\zeta \to 0$ is,

$$A(\zeta) \approx \left(\frac{3}{\pi}\right)^{\frac{1}{3}} \zeta^{\frac{2}{3}} + \ldots, \tag{5.21}$$

which value is $\frac{3}{4}$ of that obtained by cross comparison of (5.13) and (5.14). The difference is due to taking account in (5.21) in an average sort of way the effects of higher orders in k_1^2. The asymptotic behavior when $\zeta \to \infty$ is,

$$A(\zeta) \asymp \frac{25}{3\pi}(2\zeta^2)^{-\frac{1}{3}} \tag{5.22}$$

The summary of our investigation of the exchange energy is that we will replace its effects (to leading order in y) by an effective mass given by

$$\frac{m}{m^*} = 1 + A(\zeta)y^2, \tag{5.23}$$

and include $\hat{V}(0)$. I have checked numerically the behavior of $A(\zeta)$ as defined by (5.20) over the same range of ζ as shown in Fig. 1, and this definition is nowhere negative in that range. Thus the effective mass (5.23) always obeys $m \geq m^* > 0$. Further modifications to the model could be made to insure that the Debye-Hückel and second exchange corrections [19] are reproduce in the small y limit.

The next issue is how these energies vary as y increases. The important physical effect is that when the electron-electron Coulomb energy is not negligible with respect to the thermal energy, then the electron-electron repulsion forces the electrons apart and thereby reduces the energies that depend on this interaction. There are various ways of taking this effect into account. One can use the classical turning point and just take zero density where a state is classically disallowed. What comes to much the same result, but is simpler to apply is to reduce the electron-electron density by a Gibbs weight factor, $\exp[-e^2/(rkT)]$ where r is the distance between the two electrons. This method is certainly valid in the classical limit where $\zeta \to 0$. It is important that whatever is done cause these energies to vanish in the cold, dilute limit mentioned above.

To illuminate this behavior, we next compute the electron-electron repulsive energy in the presence of the Gibbs weight factor. It is,

$$\mathcal{E}_{\mathrm{e-e}} = \left(\frac{3}{4\pi r_b^3}\right)\int_0^{r_b} d\vec{r}\,\frac{e^2}{r}\exp\left(-\frac{e^2}{rkT}\right) = \frac{3e^2}{r_b}y^4\int_{y^2}^{\infty}\frac{d\xi}{\xi^3}e^{-\xi}, \tag{5.24}$$

where the change of variables $\xi = e^2/(rkT)$ was made. For small y, by expanding the exponential we get

$$\mathcal{E}_{\mathrm{e-e}} = \frac{3e^2}{2r_b}(1 - 2y^2 + \ldots, \tag{5.25}$$

We can rearrange (5.24) to give,

$$\mathcal{E}_{\mathrm{e-e}} = \frac{3e^2}{r_b}y^{-2}e^{-y^2}\int_0^{\infty}\frac{e^{-\eta}\,d\eta}{(1+y^{-2}\eta)^3} = \frac{3e^2}{r_b}y^{-2}e^{-y^2}(1 - 3y^{-2} + \ldots, \tag{5.26}$$

for the large y behavior. This behavior at both the large and small y limits can be compactly represented by,

$$\mathcal{E}_{\mathrm{e-e}} = \frac{3e^2}{2r_b}F(y^2), \quad F(y^2) \approx e^{-y^2}\left(\frac{2+2y^2}{2+4y^2+y^4}\right), \tag{5.27}$$

where $F(y^2)$ is a damping factor for $E_{\mathrm{e-e}}$. We will apply it to E_{exch} as well. (The approximation for $F(y^2)$ in (5.27) is not necessary as it can easily be evaluated numerically, but it helps to summarize the general behavior of the damping factor and I will use it in this paper.) The damping factor has the physical interpretation of representing a hole in the electron-electron density distribution reflecting their mutual repulsion.

In addition we need to consider the modification to E_{i} when $y \neq 0$. To this end we note the the difference in the potential energy experienced by the electrons between the case where the ions are uniformly distributed and the case where the ions are fixed at the center of their spheres is given by,

$$P_i(r/r_b) = \frac{e^2}{r} - \frac{3}{4\pi r_b^3}\int_{R\leq r_b}\frac{e^2\,d\vec{R}}{|\vec{R}-\vec{r}|} = \frac{e^2}{r_b}\left[\frac{r_b}{r} - \frac{3}{2} + \frac{1}{2}\left(\frac{r}{r_b}\right)^2\right]. \tag{5.28}$$

When this potential difference is averaged over a uniform distribution of electrons in the sphere, we obtain, $E_{\mathrm{i}} = 3e^2/(10r_b)$, as before. Again, to compute the effects as y increases from zero, we will apply the corresponding Gibbs weight. Thus,

$$\mathcal{E}_{\mathrm{i}} = \frac{3}{4\pi}\int_{\rho\leq 1} d\vec{\rho}\,P_{\mathrm{i}}(\rho)\exp[-y^2 P_{\mathrm{i}}(\rho)] \tag{5.29}$$

$$= \frac{3e^2}{10r_b}\left\{10\int_{\rho\leq 1} d\vec{\rho}\left(\frac{1}{\rho} - \frac{3}{2} + \frac{1}{2}\rho^2\right)\exp\left[-y^2\left(\frac{1}{\rho} - \frac{3}{2} + \frac{1}{2}\rho^2\right)\right]\right\} = \frac{3e^2}{10r_b}g(y^2).$$

For small and large y we find,

$$g(y^2) = 1 - \frac{41}{14}y^2 + \ldots, \quad \text{and} \quad g(y^2) \asymp \sqrt{\frac{2\pi}{3}}\frac{5}{2y^3}, \tag{5.30}$$

which suggests the approximation,

$$\mathcal{E}_{\rm i} \approx \left(\frac{3e^2}{10r_b}\right)\frac{1}{1+\frac{41}{14}y^2+\frac{2}{5}\sqrt{\frac{3}{2\pi}}y^3}. \tag{5.31}$$

Again, approximation (5.31) is not necessary because $g(y^2)$ is easily computed numerically, but serves to make manifest the behavior of g and I will use it in this paper.

In order to take account of the many-body quantum effects of the electron-electron repulsion and the attractive exchange interaction, I propose a modified version of (5.1), which is temperature and density dependent. It is,

$$\begin{aligned}\frac{\hbar^2k^2}{2m^*}\phi_\lambda(\vec{r}) - \frac{i\hbar^2}{m^*}\vec{k}\cdot\vec{\nabla}\phi_\lambda(\vec{r}) - \frac{\hbar^2}{2m^*}\nabla^2\phi_\lambda(\vec{r}) - \left[\frac{e^2}{r} - \frac{3e^2}{10r_b}g(y^2)\right]\phi_\lambda(\vec{r})\\ +\frac{e^2}{r_b}F(y^2)\left[\frac{27}{10} - \frac{r^2}{2r_b^2} - 2\zeta^{-\frac{1}{3}}\left(\frac{3}{\pi}\right)^{\frac{1}{3}} f_{\frac{1}{2}}(z)\right]\phi_\lambda(\vec{r}) = E_\lambda(\vec{k})\phi_\lambda(\vec{r}),\end{aligned} \tag{5.32}$$

where now we define the effective mass by

$$\frac{m}{m^*} = 1 + A(\zeta)y^2F(y^2). \tag{5.33}$$

In order to define the energy per state to go into the formalism of Section II, we first solve (5.32) by the methods of Section IV for the $E_\lambda(\vec{k})$. Then we must deduct half of the contributions from the electron-electron and ion-ion interactions as otherwise we will have over counted them. Using (5.32) to eliminate the dependence on the matrix elements which involve the derivatives, we obtain,

$$\begin{aligned}\epsilon_\lambda(\vec{k}) = \left[1 - \frac{1}{2}\left(\frac{m^*}{m}\right)A(\zeta)y^2F(y^2)\right]E_\lambda(\vec{k})\\ -\frac{3e^2}{4r_b}\left[1 - \left(\frac{m^*}{m}\right)A(\zeta)y^2F(y^2)\right]F(y^2)\left[\frac{9}{5} - \frac{1}{3}\langle\phi_\lambda(\vec{r})|\frac{r^2}{r_b^2}|\phi_\lambda(\vec{r})\rangle - \frac{4}{3}\left(\frac{3}{\pi\zeta}\right)^{\frac{1}{3}} f_{\frac{1}{2}}(z(\zeta))\right]\\ -\frac{1}{2}\left(\frac{m^*}{m}\right)A(\zeta)y^2F(y^2)\left[\langle\phi_\lambda(\vec{r})|\frac{e^2}{r}|\phi_\lambda(\vec{r})\rangle - \frac{3e^2}{10r_b}g(y^2)\right].\end{aligned} \tag{5.34}$$

The pressure, free energy *etc.* related to this revised equation follow directly from its energy spectrum (5.34) and its derivatives by (2.5 - 2.9). These derivatives are discussed in appendix A. The solution for this energy spectrum will be discussed in appendix B, and in the next section.

These results may be generalized to ions of charge Z accompanied by Z electrons each. We begin this discussion with the extension of (5.1) to $Z > 1$. Again we use the Heitler-London atomic approximation which will be valid in the cold dilute limit. It is,

$$\sum_{j=1}^{Z}\left\{\frac{\hbar^2}{2m}\left[k^2 - 2i\vec{k}\cdot\vec{\nabla}_j - \nabla_j^2\right] - \frac{Ze^2}{r_j}\right\}\phi_\lambda(\vec{r}_1,\ldots,\vec{r}_Z) + \frac{1}{2}\sum_{j\neq l}^{Z}\frac{e^2}{|\vec{r}_l - \vec{r}_j|}\phi_\lambda(\vec{r}_1,\ldots,\vec{r}_Z)$$
$$= E_\lambda(\vec{k})\phi_\lambda(\vec{r}_1,\ldots,\vec{r}_Z), \tag{5.35}$$

where $\vec{\nabla}_j$ means differentiation with respect to $\vec{r}_j$. The same value of $\vec{k}$ is used in $\exp(i\vec{k}\cdot\vec{r}_j)$ for all the $\vec{r}_j$ in order to maintain the anti-symmetry of the wave function. Of course, ϕ is meant to embody the spin-states of the electrons as well.

When the eigenspectrum is substituted into to the formalism of Section II, it is to be remembered that what is counted in (2.5) is the average number of occupied states, not the number of electrons, so N remains unity. For example, in the case of the ideal gas (non-interacting electrons) consider enlarging the cell so that it contains Z electrons. If we still consider single electron states, then for large ζ (picks out the ground state) we need $N = Z$ to allow us to occupy the lowest Z levels which we need to do in order to satisfy the exclusion principal. On the other hand, if we consider anti-symmetric states of the whole system of Z electrons, then the lowest energy state already involves the first Z single particle states and so we get the same physical ground state selected by choosing $N = 1$ in this case. Consequently, here we select cells that contain (on the average) one ion and its attendant Z electrons, and choose $N = 1$.

Following the procedures above, we now need to "correct" (5.35) to take proper account of the behavior deduced from many-body perturbation theory in the hot, dense limit. The generalized versions of $E_{\rm i}$ and $\tilde{V}$ with the damping factors included are

$$E_i = \frac{3Z^2e^2}{10r_b}g(Zy^2), \quad \text{and} \quad \tilde{V}(\vec{r}_1,\ldots,\vec{r}_Z) = \frac{3e^2}{2r_b}F(y^2)\left[Z - \frac{1}{3}\sum_{j=1}^{Z}\left(\frac{r_j}{r_b}\right)^2\right] + \frac{6Z^2e^2}{5r_b}F(y^2Z^2). \tag{5.36}$$

The generalized results for the exchange energy are given by defining $A(\zeta)$ through an equation similar to (5.19) as,

$$-\frac{e^2}{\pi Z r_b}\left(\frac{3}{\pi}\right)^{\frac{1}{3}}\zeta^{-\frac{4}{3}}X(Z\zeta) = -\frac{2e^2}{r_b}\zeta^{-\frac{1}{3}}\left(\frac{3}{\pi}\right)^{\frac{1}{3}} f_{\frac{1}{2}}(z(\zeta Z)) + \frac{3}{2}kT\zeta^{-1}y^2A(\zeta)f_{\frac{5}{2}}(z(\zeta Z)), \tag{5.37}$$

where the value ζZ replaces the value ζ in the definition (3.1) of z. The solution of (5.37) is

$$A(\zeta) = \frac{2}{3}\zeta^{\frac{2}{3}}\left(\frac{3}{\pi}\right)^{\frac{1}{3}}\left\{\frac{2f_{\frac{1}{2}}(z(Z\zeta)) - X(Z\zeta)/(\pi Z\zeta)}{f_{\frac{5}{2}}(z(Z\zeta))}\right\}. \tag{5.38}$$

With these generalizations to $Z > 1$, we propose the modified version of (5.35),

$$\begin{aligned}
&\sum_{j=1}^{Z}\left\{\frac{\hbar^2}{2m^*}\left[k^2 - 2i\vec{k}\cdot\vec{\nabla}_j - \nabla_j^2\right] - \frac{Ze^2}{r_j} + \frac{3Ze^2}{10r_b}g(Zy^2)\right\}\phi_\lambda(\vec{r}_1,\ldots,\vec{r}_Z)\\
&+\left\{\frac{1}{2}\sum_{j\neq l}^{Z}\frac{e^2}{|\vec{r}_l - \vec{r}_j|} + \frac{3e^2}{2r_b}F(y^2)\left[Z - \frac{1}{3}\sum_{j=1}^{Z}\left(\frac{r_j}{r_b}\right)^2 - \frac{4}{3}\left(\frac{3}{\pi\zeta}\right)^{\frac{1}{3}} f_{\frac{1}{2}}(z(Z\zeta))\right]\right\}\phi_\lambda(\vec{r}_1,\ldots,\vec{r}_Z)\\
&\qquad + \frac{6Z^2e^2}{5r_b}F(y^2Z^2)\phi_\lambda(\vec{r}_1,\ldots,\vec{r}_Z) = E_\lambda(\vec{k})\phi_\lambda(\vec{r}_1,\ldots,\vec{r}_Z),
\end{aligned} \tag{5.39}$$

where m^* is again given by (5.33), with $A(\zeta)$ now given by (5.38). Finally we need the generalized expression for the $\epsilon_\lambda(\vec{k})$. It is

$$\begin{aligned}
\epsilon_\lambda(\vec{k}) &= \left[1 - \frac{1}{2}\left(\frac{m^*}{m}\right)A(\zeta)y^2F(y^2)\right]E_\lambda(\vec{k})\\
&-\frac{3e^2}{4r_b}\left[1 - \left(\frac{m^*}{m}\right)A(\zeta)y^2F(y^2)\right]\left\{F(y^2)\left[Z - \frac{1}{3}\sum_{j=1}^{Z}\langle\phi_\lambda(\vec{r}_1,\ldots,\vec{r}_Z)|\frac{r_j^2}{r_b^2}|\phi_\lambda(\vec{r}_1,\ldots,\vec{r}_Z)\rangle\right.\right.\\
&\qquad\left.\left. -\frac{4}{3}\left(\frac{3}{\pi\zeta}\right)^{\frac{1}{3}} f_{\frac{1}{2}}(z(Z\zeta))\right] + \frac{4}{5}Z^2F(Z^2y^2)\right\}\\
&\qquad -\frac{1}{2}\left(\frac{m^*}{m}\right)A(\zeta)y^2F(y^2)\left[\sum_{j=1}^{Z}\langle\phi_\lambda(\vec{r}_1,\ldots\vec{r}_Z)|\frac{e^2}{r_j}|\phi_\lambda(\vec{r}_1,\ldots,\vec{r}_Z)\rangle\right.\\
&\qquad\left. -\frac{1}{2}\sum_{j\neq l}^{Z}\langle\phi_\lambda(\vec{r}_1,\ldots\vec{r}_Z)|\frac{e^2}{|\vec{r}_j - \vec{r}_l|}|\phi_\lambda(\vec{r}_1,\ldots,\vec{r}_Z)\rangle - \frac{3Ze^2}{10r_b}g(Zy^2)\right]
\end{aligned} \tag{5.40}$$

These equations are intrinsically more difficult to solve than the ones for $Z = 1$, and I shall not take up this subject here.

VI. SPHERICAL CELLULAR MODEL FOR HYDROGEN

The basic equations for our spherical cellular model for hydrogen were derived in the previous section. I take note that this model has not been refined to take account of physically relevant molecular hydrogen nor does it take account of any solid crystalline phase. It looks to only the gas and fluid phases. The purpose is not to investigate solid hydrogen, as there is already a great body of work on this topic. The molecular states which are very relevant physically could be included by including two protons and two electrons in each cell, but the theoretical structure requires some modification and the numerical work increases significantly. This extension will not be part of the present work. For numerical purposes, it is convenient to rewrite the basic equations in terms of

$$\mathcal{E}_{l,\lambda}(\vec{k}) = E_{l,\lambda}(\vec{k}) - \frac{3e^2}{10r_b}g(y^2) - \frac{e^2}{r_b}F(y^2)\left[\frac{27}{10} - 2\left(\frac{3}{\pi\zeta}\right)^{\frac{1}{3}} f_{\frac{1}{2}}(z(\zeta))\right]. \tag{6.1}$$

The subscript (λ) has been expanded here to (l,λ) to emphasis the resolution of the eigenfunctions in spherical coordinates. Thus (5.32) becomes,

$$\frac{\hbar^2 k^2}{2m^*}\phi_\lambda(\vec{r}) - \frac{i\hbar^2}{m^*}\vec{k}\cdot\vec{\nabla}\phi_\lambda(\vec{r}) - \frac{\hbar^2}{2m^*}\nabla^2\phi_\lambda(\vec{r}) - \left[\frac{e^2}{r} + \frac{e^2r^2}{2r_b^3}F(y^2)\right]\phi_\lambda(\vec{r}) = \mathcal{E}_{l,\lambda}(\vec{k})\phi_\lambda(\vec{r}), \tag{6.2}$$

and (5.34) becomes,

$$\begin{aligned}\epsilon_{l,\lambda}(\vec{k}) = \frac{1}{2}\left(1+\frac{m^*}{m}\right)\mathcal{E}_{l,\lambda}(\vec{k}) + \frac{3e^2}{10r_b}g(y^2) + \frac{e^2}{r_b}F(y^2)\left[\frac{27}{20} - \left(\frac{3}{\pi\zeta}\right)^{\frac{1}{3}} f_{\frac{1}{2}}(z(\zeta))\right] \\ + \langle\phi_{l,\lambda}(\vec{r})|\left\{-\frac{e^2}{2r} + \frac{m^*}{2m}\left[\frac{e^2}{r} + \frac{e^2r^2}{2r_b^3}F(y^2)\right]\right\}|\phi_{l,\lambda}(\vec{r})\rangle,\end{aligned} \tag{6.3}$$

where g, F and m^* are given by (5.20), (5.26), (5.27), (5.29), (5.31) and (5.33).

Next we follow the procedures used for the spherical cellular model of an ideal gas developed in Sec. IV, except the starting guess for μ is now taken to be $5kT$ plus the lowest eigenvalue. We treat $H' = -(i\hbar^2/m^*)\vec{k}\cdot\vec{\nabla}$ as a perturbation, and solve the rest of the equation as resolved in spherical coordinates. In order to apply these methods, it is necessary to extend the computation of the root mean square deviation of the eigenvalues over each nearly degenerate block to our present case. In Appendix B we discuss the character of the

degeneracy structure of (6.2) with $|\vec{k}| = 0$. There we find that the states are divided into ideal-gas-like states, jumper states, and Coulomb-like states. Again, as in Sec. IV, we will use ω to denote the ωth excited state, that is the $\omega + 1$st level.

For the ideal-gas-like states ($\omega + 1 > \sigma$ with σ defined in Appendix B), (4.21) continues to be valid with m^* replacing m. For uniformity, the subscript ω to Δ will be replaced by (l, n). For the case of the Coulomb-like states ($\omega + 1 \leq \sigma$), if we define $\tilde{L}$ to be the lesser of the maximum value of l considered and $\omega = n + l$, then in this regime,

$$\left[\frac{\hbar^2 k_B^2}{2m^*}\Delta_{l,n}(k)\right]^2 = \frac{4}{(\tilde{L}+1)^2}\left(\frac{\hbar^2 k^2}{2m^*}\right)\sum_{l'=0}^{\tilde{L}}\left(\frac{2l'+1}{3}\right)T_{l',\omega-l'}. \tag{6.4}$$

Finally, for the jumper states,

$$\left[\frac{\hbar^2 k_B^2}{2m^*}\Delta_{l,n}(k)\right]^2 = \frac{8}{\sigma(\sigma+1)(2\sigma+1)}\left(\frac{\hbar^2 k^2}{2m^*}\right)\sum_{(l',\omega)\in\mathcal{J}}\left(\frac{2l'+1}{3}\right)T_{l',\omega}, \tag{6.5}$$

where the set $\mathcal{J}$ is defined by equation (B11) in the Appendix B. If all the jumper states are not included because the maximum value of l considered is too small, then this equation would have to be modified; however, the approximation to the physical situation would then be rather poor so we will not elaborate on this case.

This model is defined by (4.22) and (2.9), which is made explicit in (4.23) for the ideal gas case. Here we need to use,

$$e_{l,n} = \frac{2m\epsilon_{l,n}(\vec{0})}{\hbar^2 k_B^2} \tag{6.6}$$

with the $\epsilon_{l,n}$ defined by (6.3). The derivative of $\mathcal{E}_{l,n}$ with respect to r_b is given by (A5). For the complete evaluation of the derivatives necessary to put in the numerator of (2.9), we need the derivatives of m^*, $g(y^2)$, $F(y^2)$ and $(3/\pi\zeta)^{\frac{1}{3}} f_{\frac{1}{2}}(z(\zeta))$, as well as of course $1/r_b$, with respect to r_b. The best method is to compute these quantities directly from their definitions by a direct numerical evaluation. I shall however in this paper simply differentiate the representations previously given. This procedure will insure thermodynamic consistency, at the cost of some possible loss in accuracy. Finally we need the derivative of the matrix element appearing in (6.3). This result is given by (A11). All these parts may be assembled into a rather length expression for the numerator of (2.9) appropriate for this case. We take,

$$\mathcal{E}_{l,\lambda}(\vec{k}) = \mathcal{E}_{l,\lambda}(\vec{0}) + \frac{\hbar^2 k^2}{2m^*} \pm \frac{\hbar^2 k_B^2}{2m^*}\Delta_{l,\lambda}(k), \tag{6.7}$$

where the $\pm$ is for the two energy values for each $|\vec{k}|$ that we used as the method to take account of all the different directions of $\vec{k}$ in Sec. IV. We will use the same method here for the same purpose. If we differentiate (6.3), use (6.7) and (A5), then we get,

$$\begin{aligned}
r_b \frac{\partial}{\partial r_b}\epsilon_{l,\lambda}(\vec{k}) = &-\frac{1}{2}\left(1+\frac{m^*}{m}\right)\left\{\left(2+\frac{\partial \log m^*}{\partial \log r_b}\right)\left[\mathcal{E}_{l,\lambda}(\vec{0}) + \frac{\hbar^2 k^2}{2m^*} \pm \frac{\hbar^2 k_B^2}{2m^*}\Delta_{l,\lambda}(k)\right]\right. \\
&\left. -\langle\phi_{l,\lambda}(\vec{r})|\left[\frac{e^2 r^2}{2r_b^3}y^2 F'(y^2) - \left(1+\frac{\partial \log m^*}{\partial \log r_b}\right)\left(\frac{e^2}{r}+\frac{e^2 r^2}{2r_b^3}F(y^2)\right)\right]|\phi_{l,\lambda}(\vec{r})\rangle\right\} \\
&+\frac{1}{2m}\frac{\partial m^*}{\partial \log r_b}\left[\mathcal{E}_{l,\lambda}(\vec{0}) + \frac{\hbar^2 k^2}{2m^*} \pm \frac{\hbar^2 k_B^2}{2m^*}\Delta_{l,\lambda}(k)\right] - \frac{e^2}{r_b}\left\{\frac{3}{10}g(y^2) + \frac{3}{10}y^2 g'(y^2)\right. \\
&\left. +\frac{27}{20}[F(y^2)+y^2F'(y^2)] - y^2F'(y^2)\left(\frac{3}{\pi\zeta}\right)^{\frac{1}{3}} f_{\frac{1}{2}}(z(\zeta)) - 3\left(\frac{3}{\pi\zeta}\right)^{\frac{1}{3}}\zeta f'_{\frac{1}{2}}(z(\zeta))F(y^2)\right\} \\
&+r_b\frac{\partial}{\partial r_b}\langle\phi_{l,\lambda}(\vec{r})|\left\{-\frac{e^2}{2r}+\frac{m^*}{2m}\left[\frac{e^2}{r}+\frac{e^2 r^2}{2r_b^3}F(y^2)\right]\right\}|\phi_{l,\lambda}(\vec{r})\rangle,
\end{aligned} \tag{6.8}$$

where the last line is given by (A11). These equations have been programmed in the same manner as described for those of Sec. IV.

The are several features which are expected from this model. First, if the temperature is sufficiently high, the electron will be mostly in the high energy states which are very much like those for the free electron gas. This feature is the so called "hot curve" limit. As an illustration of this behavior, we display in Fig. 3 the ratio of the electron pressure to the ideal electron gas pressure for a temperature of 1000 electron volts, as a function of density. (The plot is versus ζ for easy of comparison with Fig. 1.) A line for the ratio exactly equal to unity is put in to guide the eye. The fluctuations about this line are reminiscent of those in Fig. 1. The values of the pressure ratio greater than unity are undoubtedly due to the spherical approximation, as was the case in the spherical cellular model approximation to the ideal gas.

Another feature which is to be expected is that when the temperature is low enough the dominant feature is the repulsive pressure exerted by the compressed atoms as the density is increased. This feature is the so called "cold curve" limit. The resulting pressure is roughly

independent of the temperature. We plot in Fig. 4, the results for several temperatures. The ratio to the Thomas-Fermi cold curve is what is plotted. I have used the representation of Baker and Johnson [36]. It is, for reference,

$$P_{\text{cold curve}} = 9.0549692 \left(\frac{w}{\rho}\right)^{5/3} \left[\frac{(1 + 1.59659x^{a_-} + 1.06595x^{2a_-})}{1 + 0.2783436x^{-a_-}}\right]^{9.715}, \tag{6.9}$$

in megabars where x is given by (4.26), ρ is the density in grams per cubic centimeter, w is the gram molecular weight, and $a_- \approx -0.772$. It is to be noticed that the cold curve produced by this model is lower than that of the Thomas-Fermi model, which latter is known [3] to be too high, except in the limit of infinite density where both models reduce to the high density ideal electron gas. As the temperature increases, the pressure begins to deviate from the cold curve at successively higher densities.

The spherical cellular model of hydrogen predicts a phase transition. This fact can be seen, for example, by plotting the total pressure (the electron pressure plus the pressure associated with the motion of the center of mass of the atom) versus the volume for $T = 1.5$ ev. This plot is given as Fig. 5 as the solid curve. The region where the pressure increases with the volume is physically unstable. The dotted line represent the pressure derived from the Maxwell construction which corresponds to a tangent line in the plot of the Gibbs Free energy to maintain its convexity property. I take this opportunity to show some of the effects of the many-body terms. The dashed curve is just the Heitler-London atom (with our boundary conditions) and it omits the many-body terms. The line of short dashes shows the Maxwell construction for that curve. The pressure-volume plot with the tie-lines drawn in is given in Fig. 6. The critical properties of this model are: $T_c \approx 1.83$ ev., $\rho_c \approx 0.11$ gm/cc., $P_c \approx 0.084$ MB, $\zeta_c \approx 4.4$, and $y_c \approx 2.3$. These values are at considerable variance with the experimental values for the liquid gas critical point in hydrogen, which are roughly 33° K, 12.8 atmospheres and 0.03 gm/cc. Since there is no provision in the model as yet for two-atom molecular states, perhaps this difference is not surprising. A V-T plot and a P-T plot of the phase boundary is given in Fig. 7.

Margo *et al.* find a critical point at about half the temperature and and twice the density

of that given here. They indicate that they believe that there phase transition is related to the molecular dissociation. Thus it is worth while to consider the nature of the phase transition in the spherical cellular model of hydrogen. One method is to consider the pressure along the phase boundary. We have plotted in Fig. 8 the total pressure divided by the sum of the ideal electron gas pressure and the pressure due to the center of mass motion of the electron and the proton. At least for low densities, if the system consists of hydrogen atoms, this quantity should be about one-half. A dotted line has been included at this level in Fig. 8 to guide the eye. A ratio of about one-quarter would be expected in the presence of molecular hydrogen. Pressure ratios higher than one-half would be indicative of ionization. Lower pressure ratios would presumable indicate the formation of groups of atoms bound together. What we see is that on the high density (small V) side of the critical point, the pressure decrease very rapidly, which probably indicates a condensed state. On the low density side, the pressure ratio rises to about 0.69, and then declines. Another way to investigate the nature of the transition is to plot the internal energy along an isotherm which intersects the two phase-region. Such a figure for $T = 0.5$ ev. is shown in Fig. 9. A dotted line has been added at the lowest energy level of atomic hydrogen. Here we see that in the high-density region that as the density decreases toward the phase boundary (indicated by a dot) the internal energy drops below that of atomic hydrogen due to the many body interactions which suggest a bound many-body state of the system. The model produces a continuous curve through the two-phase region which is shown. On the low-density side, the energy is higher than that of atomic hydrogen and suggest the existence of some excited states, and perhaps a bit of ionization. Continuing to even lower densities there is again binding energy which is greater than that of atomic hydrogen. I have illustrated the effects of the many-body terms by including a dashed curve which omits them. As also seen in Fig. 5, the deviations from the Heitler-London atom become apparent when the system becomes mostly plasma like. The pressure ratio of Fig. 8 indeed for $T = 0.5$ ev. drops to a minimum of about 0.33 at a volume of about 8000 cc/gm. and then begins to increase again. This increase is to be expected as one expects total ionization [41] in the infinitely dilute limit for

fixed temperature. One can see this effect more clearly in the energy ratio plot for $T = 10$ ev. given in Fig. 10. Also note in this figure that in the high density limit, the increase in the free electron energy (and pressure) due to the Pauli exclusion principle swamps the effects of the Coulomb interaction and again leads to U_{ideal} as the asymptotic value of U_{electron}. We conclude that the phase transition found to occur in this model is best described as a localization-delocalization transition.

One further question of interest is the low-density ionization profile predicted by this model. The Saha formula [42] suggests that

$$Z_{\text{i}} = \frac{1}{1 + A\zeta \exp(\chi/T)}, \tag{6.10}$$

where A is a constant, and $\chi = 13.5978$ ev. is the ionization potential for atomic hydrogen. For isochores, this equation suggests a plot against $1/T$ would be appropriate. I give such a plot in Fig. 11 for four different densities. The curves could be extended to the phase boundaries, but they are most relevant to ionization behavior while they are positive. Even here the pressure probably understates the degree of ionization, as there may well be some clumping of atoms which would give a negative contribution to the electron pressure. This issue requires further investigation.

ACKNOWLEDGMENTS

The author is pleased to acknowledge many helpful conversations with J. J. Erpenbeck, M. E. Fisher, J. D. Johnson, and W. W. Wood.

REFERENCES

[1] L. H. Thomas, Proc. Camb. Philos. Soc. **23**, 542 (1927).

[2] E. Fermi, Rend. Accad. Naz. Lincei **6**, 602 (1927).

[3] R. P. Feynman, N. Metropolis and E. Teller, Phys. Rev. **75**, 1561 (1949).

[4] E. Lieb, Rev. Mod. Phys. **53**, 603 (1981).

[5] R. G. Parr and W. Yang, *Density-Functional Theory of Atoms and Molecules*, (Oxford University Press, New York, 1989).

[6] L. Spruch, Rev. Mod. Phys. **63**, 151 (1991).

[7] P. A. M. Dirac, Proc. Camb. Philos. Soc. **26**, 376 (1930).

[8] R. D. Cowan and J. Ashkin, Phys. Rev. **105**, 144 (1957).

[9] P. Debye and E. Hückel, Phys. Z. Sowjetunion **24**, 185 (1923).

[10] M. E. Fisher and Y. Levin, Phys. Rev. Letts. **71**, 3826 (1993).

[11] Y. Levin and M. E. Fisher, Physica **A 225**, 164 (1996).

[12] B. P. Lee and M. E. Fisher, Phys. Rev. Letts. **76**, 2906 (1996).

[13] N. F. Carnahan and K. E. Starling, J. Chem. Phys. **51**, 635 (1969).

[14] G. A. Mansoori, N. F. Carnahan, K. E. Starling, and T. W. Leland, J. Chem. Phys. **54**, 1523 (1971).

[15] J. A. Barker and D. Henderson, Rev. Mod. Phys. **48**, 597 (1976).

[16] J. D. Weeks, D. Chandler, and H. C. Andersen, Adv. Chem. Phys. **34**, 105 (1976).

[17] G. A. Baker, Jr., M. de Llano, and J. Pineda, Phys. Rev. **B 24**, 6304, and references therein.

[18] C. Keller, M. de Llano, S. Z. Ren, M. A. Solis, and G. A. Baker, Jr., Annals of Phys.

251, 64 (1996).

[19] G. A. Baker, Jr. and J. D. Johnson in *Condensed Matter Theories*, M. Cassas, M. de Llano, J. Navarro, and A. Polls, eds. Vol. 10, pg. 173 (Nova Science Pub. Inc., Commack, NY, 1995).

[20] F. H. Ree, J. Chem. Phys. **73**, 5401 (1980).

[21] J. J. Nicolas, K. E. Gubbins, W. B. Streett. and D. J. Tildesley, Mol. Phys. **37**, 1429 (1979).

[22] J. K. Johnson, J. A. Zollweg, and K. E. Gubbins, Mol. Phys. **78**, 591 (1993).

[23] A. Bunker, S. Nagel, R. Redmer, and G. Röpke, Phys. Rev. **B**, in press.

[24] W.-D. Kraeft, D. Kremp, W. Ebeling, and G. Röpke, *Quantum Statistics of Charged Particle Systems* (Akademie-Verlag, Berlin, 1986).

[25] D. Kremp, W.-D. Kraeft, and M. Schlanges, Contrib. Plasma Phys. **33**, 567 (1993).

[26] W. Ebeling, A. Förster, H. Hess, and M. Y. Romanovsky, Plasma Phys. & and Contr. Fusion **38**, A31 (1996).

[27] H. C. Graboske, Jr., D. J. Harwood, and F. J. Rodgers, Phys. Rev. **186**. 210 (1969).

[28] V. E. Fortov and V. K. Gryaznov in *Strongly Coupled Plasma Physics*, edited by F. J. Rodgers and H. E. Dewitt (Plenum Press, New York, 1987), pg. 87.

[29] G. A. Baker, Jr., *Condensed Matter Theories* **11**, to be published.

[30] See, for example, P. W. Anderson, *Concepts in Solids, Lectures on the Theory of Solids*, (Benjamin, Reading, Mass., 1963).

[31] W. R. Magro, D. M. Ceperley, C. Pierleoni, and B. Bernu, Phys. Rev. Lett. **76**, 1240 (1996).

[32] M. Gell-Mann and K. A. Brueckner, Phys. Rev. **106**, 364 (1957).

[33] E. P. Wigner and F. Seitz, Phys. Rev. **43**, 804 (1933); **46**, 509 (1934).

[34] K. Huang, *Statistical Mechanics* (Wiley, New York, 1963).

[35] N. W. Ashcroft and N. D. Mermin, *Solid State Physics* (Holt, Rinehart and Winston, New York, 1976).

[36] G. A. Baker, Jr. and J. D. Johnson, Phys. Rev. **A 44**, 2271 (1991).

[37] M. Abramowitz and I. A. Stegun, *Handbook of Mathematical Functions* Nat. Bureau of Stand. AMS **55** (US Govt. Printing Office, Washington, 1964).

[38] P. M. Morse and H. Feshbach, *Methos of Theoretical Physics*, Vol. II, p. 1576 (McGraw-Hill, New York, 1953).

[39] J. Bardeen, J. Chem. Phys. **6**, 367 (1938)

[40] See, for example, A. A. Abrikosov, L. P. Gorkov and I. E. Dzyaloshinski, *Methods of Field Theory in Statistical Physics* as transl. by R. A. Silverman (Prentice-Hall, Englewood Cliffs, N. J., 1963).

[41] J. L. Lebowitz and R. E. Peña, J. Chem. Phys. **59**, 1362 (1973).

[42] N. H. Saha, Phil. Mag. **40**, 472 (1920); D. Mihalas, *Stellar Atmospheres* (W. H. Freeman, San Francisco, 1970).

APPENDIX A: ENERGY DERIVATIVES

In order to use (2.9) it is convenient to re-express $\partial\epsilon_j/\partial r_b$ in terms of the wave function. First note that for $\vec{k}$ in the first Brillouin zone, it is to be remembered that $\vec{k}$ can be parameterized as $\vec{k} = \vec{\kappa}/r_b$ with $\vec{\kappa}$ independent of the cell size. Also we will use $\vec{r} = r_b\vec{\rho}$ and the derivatives $\vec{\nabla}$ and ∇^2 are to be taken here with respect to $\vec{\rho}$. In this notation, (6.2) becomes

$$\frac{\hbar^2}{2m^* r_b^2}\left(\kappa^2 - 2i\vec{\kappa}\cdot\vec{\nabla} - \nabla^2\right)\phi(r_b,\vec{\rho}) + V(r_b,\vec{\rho})\phi(r_b,\vec{\rho}) = \mathcal{E}\phi(r_b,\vec{\rho}). \tag{A1}$$

If we now differentiate with respect to r_b, and denote the partial with respect to r_b by an over dot, we get,

$$\begin{aligned}
&-\frac{\hbar^2}{2m^* r_b^2}\left(\frac{2}{r_b} + \frac{\dot{m}^*}{m^*}\right)\left(\kappa^2 - 2i\vec{\kappa}\cdot\vec{\nabla} - \nabla^2\right)\phi(r_b,\vec{\rho}) + \dot{V}(r_b,\vec{\rho})\phi(r_b,\vec{\rho}) \\
&+\frac{\hbar^2}{2m^* r_b^2}\left(\kappa^2 - 2i\vec{\kappa}\cdot\vec{\nabla} - \nabla^2\right)\dot{\phi}(r_b,\vec{\rho}) + [V(r_b,\vec{\rho}) - \mathcal{E}]\dot{\phi}(r_b,\vec{\rho}) = \dot{\mathcal{E}}\phi(r_b,\vec{\rho}).
\end{aligned} \tag{A2}$$

The next step is to multiply (A2) by $\phi^*(r_b,\vec{\rho})d\vec{r}$ and integrate over the unit cell. The result is,

$$\begin{aligned}
&-\left(\frac{2}{r_b} + \frac{\dot{m}^*}{m^*}\right) r_b^3 \int d\vec{\rho}\,\phi^*(r_b,\vec{\rho})\left\{\frac{\hbar^2}{2m^* r_b^2}\left(\kappa^2 - 2i\vec{\kappa}\cdot\vec{\nabla} - \nabla^2\right)\phi(r_b,\vec{\rho}) + V(r_b,\vec{\rho})\phi(r_b,\vec{\rho})\right\} \\
&\qquad + r_b^3 \int d\vec{\rho}\,\phi^*(r_b,\vec{\rho})\left[\dot{V}(r_b,\vec{\rho}) + \left(\frac{2}{r_b} + \frac{\dot{m}^*}{m^*}\right)V(r_b,\vec{\rho})\right]\phi(r_b,\vec{\rho}) + \\
&r_b^3 \int d\vec{\rho}\,\phi^*(r_b,\vec{\rho})\left\{\frac{\hbar^2}{2m^* r_b^2}\left(\kappa^2 - 2i\vec{\kappa}\cdot\vec{\nabla} - \nabla^2\right)\dot{\phi}(r_b,\vec{\rho}) + [V(r_b,\vec{\rho}) - \mathcal{E}]\dot{\phi}(r_b,\vec{\rho})\right\} = \dot{\mathcal{E}},
\end{aligned} \tag{A3}$$

where use has been made of the normalization of ϕ. If we now use (A1) on the first line of (A3), integrate by parts in the last line so that the derivatives act on ϕ^* instead of $\dot{\phi}$, and use (A1) again, we get

$$\begin{aligned}
\dot{\mathcal{E}} = &-\left(\frac{2}{r_b} + \frac{\dot{m}^*}{m^*}\right)\mathcal{E} + r_b^3 \int d\vec{\rho}\,\phi^*(r_b,\vec{\rho})\left[\dot{V}(r_b,\vec{\rho}) + \left(\frac{2}{r_b} + \frac{\dot{m}^*}{m^*}\right)V(r_b,\vec{\rho})\right]\phi(r_b,\vec{\rho}) \\
&-\frac{\hbar^2 r_b}{2m^*}\int dS\,\vec{n}\cdot\left[\phi^*(r_b,\vec{\rho})\vec{\nabla}\dot{\phi}(r_b,\vec{\rho}) - \dot{\phi}(r_b,\vec{\rho})\vec{\nabla}\phi^*(r_b,\vec{\rho}) + 2i\vec{\kappa}\phi^*(r_b,\vec{\rho})\dot{\phi}(r_b,\vec{\rho})\right],
\end{aligned} \tag{A4}$$

where $\int dS$ is over the surface of the cell and $\vec{n}$ is the outward pointing normal. The last line in (A4) vanishes because of the periodicity. That is to say, the value of the ϕ's is the

same on opposite sides of the cell, but the normal vector $\vec{n}$ points in opposite directions, so these contributions cancel each other. Thus we conclude that,

$$r_b \frac{\partial \mathcal{E}}{\partial r_b} = -\left(2 + \frac{\partial \log m^*}{\partial \log r_b}\right) \mathcal{E}$$
$$+ r_b^3 \int d\vec{\rho}\, \phi^*(r_b, \vec{\rho}) \left[r_b \dot{V}(r_b, \vec{\rho}) + \left(2 + \frac{\partial \log m^*}{\partial \log r_b}\right) V(r_b, \vec{\rho}) \right] \phi(r_b, \vec{\rho}). \tag{A5}$$

We really need $\partial \epsilon_{l,\lambda} / \partial r_b$, so in addition, we need, by (6.3) to differentiate the further term.

$$\frac{\partial}{\partial r_b} \langle \phi_{l,\lambda}(\vec{r}) | \left\{ -\frac{e^2}{2r} + \frac{m^*}{2m} \left[\frac{e^2}{r} + \frac{e^2 r^2}{2 r_b^3} F(y^2) \right] \right\} | \phi_{l,\lambda}(\vec{r}) \rangle = \tag{A6}$$
$$\langle \phi | \{\mathcal{V}\} | \dot{\phi} \rangle + \langle \phi | \left\{ \dot{\mathcal{V}} \right\} | \phi \rangle + \langle \dot{\phi} | \{\mathcal{V}\} | \phi \rangle,$$

schematically. This formula requires the values of $\dot{\phi}(r_b, \vec{\rho})$. If we substitute the results of (A5) in (A2), then we get an inhomogeneous differential equation for $\dot{\phi}(r_b, \vec{\rho})$. The boundary conditions (in spherical coordinates) are easier to describe if we make the usual substitution, $u(r_b, \vec{\rho}) = r_b \rho \phi(r_b, \vec{\rho})$. Then, necessarily $\dot{u}(r_b, \vec{0}) = 0$. For the case of odd parity states, we also must have $\dot{u}(r_b, r_b) = 0$. For even parity, $\partial \phi(r_b, r)/\partial r|_{r=r_b} = 0$ implies that $\rho \partial u(r_b, \rho)/\partial \rho|_{\rho=1} = u(r_b, \rho)|_{\rho=1}$, which, by taking the partial with respect to r_b, gives directly the remaining boundary condition that $\partial \dot{u}(r_b, \rho)/\partial \rho|_{\rho=1} = \dot{u}(r_b, \rho)|_{\rho=1}$ for states of even parity. As these boundary conditions are the same as for the eigenfunction solutions of (A1), we may expand,

$$\frac{\partial \phi_{l,\lambda}(r_b . \vec{\rho})}{\partial r_b} = \sum_{\nu \neq \lambda} a_{l,\nu} \phi_{l,\nu}(r_b, \vec{\rho}). \tag{A7}$$

To express the solution, it is convenient to define the quantities,

$$V_\nu(l, \lambda) = \frac{e^2}{r_b} \langle \phi_{l,\nu}(r_b, \vec{\rho}) | \rho^{-1} | \phi_{l,\lambda}(r_b, \vec{\rho}) \rangle \qquad H_\nu(l, \lambda) = \frac{e^2}{r_b} \langle \phi_{l,\nu}(r_b, \vec{\rho}) | \rho^2 | \phi_{l,\lambda}(r_b, \vec{\rho}) \rangle \tag{A8}$$

The next step is to substitute (A7) into (A2), to multiply on the left by $\phi^*_{l,\nu}(r_b, \vec{\rho}) d\vec{r}$ for $\nu \neq \lambda$ and to integrate over the cell. If use (A1), we can eliminate the derivative and the explicitly $\vec{k}$ dependent terms. The result is,

$$(\mathcal{E}_{l,\lambda}-\mathcal{E}_{l,\nu})a_{l,\nu}=\frac{e^2}{r_b}\langle\phi_{l,\nu}(r_b,\vec{\rho})|\left[\frac{\rho^2y^2}{2r_b}F'(y^2)-\left(\frac{1}{r_b}+\frac{\dot{m}^*}{m^*}\right)\left(\frac{1}{\rho}+\frac{1}{2}\rho^2F(y^2)\right)\right]|\phi_{l,\lambda}(r_b,\vec{\rho})\rangle. \tag{A9}$$

Thus,

$$\begin{aligned}r_b\frac{\partial\phi_{l,\lambda}(r_b,\vec{\rho})}{\partial r_b}=\sum_{\nu\neq\lambda}\frac{\phi_{l,\nu}(r_b,\vec{\rho})}{\mathcal{E}_{l,\nu}-\mathcal{E}_{l,\lambda}}\Bigg\{&\left(1+\frac{\partial\log m^*}{\partial\log r_b}\right)V_\nu(l,\lambda)\\&+\frac{1}{2}\left[\left(1+\frac{\partial\log m^*}{\partial\log r_b}\right)F(y^2)-y^2F'(y^2)\right]H_\nu(l,\lambda)\Bigg\}.\end{aligned} \tag{A10}$$

The substitution of (A10) into (A6) gives, for the needed case $\vec{k}=\vec{0}$ where V and H are real, the result,

$$\begin{aligned}r_b\frac{\partial}{\partial r_b}\langle\phi_{l,\lambda}(\vec{r})|\left\{-\frac{e^2}{2r}+\frac{m^*}{2m}\left[\frac{e^2}{r}+\frac{e^2r^2}{2r_b^3}F(y^2)\right]\right\}|\phi_{l,\lambda}(\vec{r})\rangle&=\left(1+\frac{\partial\log m^*}{\partial\log r_b}\right)\left(\frac{m^*}{m}-1\right)\mathcal{A}(l,\lambda)\\&+\frac{1}{2}\left[\left(1+\frac{\partial\log m^*}{\partial\log r_b}\right)F(y^2)-y^2F'(y^2)\right]\frac{m^*}{m}F(y^2)\mathcal{B}(l,\lambda)\\+\left\{\left(1+\frac{\partial\log m^*}{\partial\log r_b}\right)\frac{m^*}{m}F(y^2)+\frac{1}{2}\left(\frac{m^*}{m}-1\right)\left[\left(1+\frac{\partial\log m^*}{\partial\log r_b}\right)F(y^2)-y^2F'(y^2)\right]\right\}\mathcal{C}(l,\lambda)&\\+\frac{1}{2}\left(1-\frac{m*}{m}\right)V_\lambda(l,\lambda)+\frac{1}{2m}\frac{\partial m^*}{\partial\log r_b}[V_\lambda(l,\lambda)+\frac{1}{2}F(y^2)H_\lambda(l,\lambda)]&\\-\frac{m^*}{4m}(F(y^2)+y^2F'(y^2))H_\lambda(l,\lambda),&\end{aligned} \tag{A11}$$

where we define the further quantities,

$$\mathcal{A}(l,\lambda)=\sum_{\nu\neq\lambda}\frac{[V_\nu(l,\lambda)]^2}{\mathcal{E}_{l,\nu}-\mathcal{E}_{l,\lambda}},\quad\mathcal{B}(l,\lambda)=\sum_{\nu\neq\lambda}\frac{[H_\nu(l,\lambda)]^2}{\mathcal{E}_{l,\nu}-\mathcal{E}_{l,\lambda}},\quad\mathcal{C}(l,\lambda)=\sum_{\nu\neq\lambda}\frac{V_\nu(l,\lambda)H_\nu(l,\lambda)}{\mathcal{E}_{l,\nu}-\mathcal{E}_{l,\lambda}}. \tag{A12}$$

Thus the substitution of the results of (A5) and (A12) into (2.9) plus some further straightforward differentiations gives via (6.3) an explicit expression for the pressure. Likewise, we obtain an explicit expression for the Gibbs free energy by means of this result and (2.10).

The computation of $\partial\epsilon_j/\partial T|_\Omega$ needed in (2.7) proceeds in a similar manner. It begins with the differentiation of (6.2) with respect to T as at (A2). The result is

$$\begin{aligned}-\frac{\partial m^*}{\partial T}\frac{\hbar^2}{2(m^*)^2}\left(k^2-2i\vec{k}\cdot\vec{\nabla}-\nabla^2\right)\phi(\vec{r})+\frac{e^2r^2}{2Tr_b^3}F'(y^2)y^2\phi(\vec{r})&\\+\frac{\hbar^2}{2m^*}\left(k^2-2i\vec{k}\cdot\vec{\nabla}-\nabla^2\right)\frac{\partial\phi(\vec{r})}{\partial T}-\left[\frac{e^2}{r}+\frac{e^2r^2}{2r_b^3}F(y^2)+\mathcal{E}\right]\frac{\partial\phi(\vec{r})}{\partial T}&=\frac{\partial\mathcal{E}}{\partial T}\phi(\vec{r}),\end{aligned} \tag{A13}$$

where use was made of $\partial(y^2)/\partial T = -y^2/T$. Again the next step is to multiply by $\phi^* d\vec{r}$ on the left and integrate over the spherical cell. As in the transition from (A3) to (A4) the operators acting on $\partial\phi/\partial T$ are, by an integration by parts made to act on ϕ^* instead and then by means of Schrödinger's equation eliminated in favor of some surface terms. These terms cancel as they did in (A4). By further use of Schrödinger's equation we can eliminate the matrix elements depending on derivatives and thus obtain,

$$T\frac{\partial\mathcal{E}}{\partial T} = -\frac{T}{m^*}\frac{\partial m^*}{\partial T}\left\{\mathcal{E} + \int d\vec{r}\,\phi^*(\vec{r})\left[\frac{e^2}{r} + \frac{e^2r^2}{2r_b^3}F(y^2)\right]\phi(\vec{r})\right\} + \frac{e^2F'(y^2)y^2}{2r_b^3}\int d\vec{r}\,\phi^*(\vec{r})r^2\phi(\vec{r}). \tag{A14}$$

The $\partial\epsilon/\partial T$ now follow by straightforward differentiation of (6.3) with respect to T. It is to be noticed that, as in (A6), the $\partial/\partial T$ of the same matrix element is also required. Again if we use the standard substitution, $u(r) = r\phi(r)$ for the radial part of the wave function, we find $\partial u/\partial T = 0$ for $r = 0$, and also for $r = r_b$ for states of odd parity. For states of even parity, the other boundary condition is

$$\frac{\partial^2 u(r)}{\partial r\partial T} = \frac{1}{r}\frac{\partial u(r)}{\partial T} \qquad \text{for } r = r_b. \tag{A15}$$

Again we find that these boundary conditions are the same as those satisfied by the eigenfunctions of (A1), so we can make the expansion,

$$\frac{\partial\phi_{l,\lambda}(r_b.\vec{\rho})}{\partial T} = \sum_{\nu\neq\lambda} b_{l,\nu}\phi_{l,\nu}(r_b,\vec{\rho}). \tag{A16}$$

Proceeding as above, we find,

$$T\frac{\partial\phi_{l,\lambda}(r_b,\vec{\rho})}{\partial T} = \tag{A17}$$
$$\sum_{\nu\neq\lambda}\frac{\phi_{l,\lambda}(r_b,\vec{\rho})}{\mathcal{E}_{l,\nu}-\mathcal{E}_{l,\lambda}}\left\{\frac{\partial\log m^*}{\partial\log T}\left[V_\nu(l,\lambda) + \frac{1}{2}F(y^2)H_\nu(l,\lambda)\right] - \frac{1}{2}y^2F'(y^2)H_\nu(l,\lambda)\right\}.$$

Thus we get, again for the needed case $\vec{k} = \vec{0}$,

$$T\frac{\partial}{\partial T}\langle\phi_{l,\lambda}(\vec{r})|\left\{-\frac{e^2}{2r} + \frac{m^*}{2m}\left[\frac{e^2}{r} + \frac{e^2r^2}{2r_b^3}F(y^2)\right]\right\}|\phi_{l,\lambda}(\vec{r})\rangle = \frac{\partial\log m^*}{\partial\log T}\left(\frac{m^*}{m} - 1\right)\mathcal{A}(l,\lambda)$$
$$+\frac{1}{2}\left[\frac{\partial\log m^*}{\partial\log T}F(y^2) - y^2F'(y^2)\right]F(y^2)\mathcal{B}(l,\lambda)$$

$$+\left[\left(\frac{m^*}{m}+1\right)\frac{\partial \log m^*}{\partial \log T}F(y^2)-\left(\frac{m^*}{m}-1\right)y^2F'(y^2)\right]\mathcal{C}(l,\lambda)$$
$$+\frac{1}{2m}\frac{\partial m^*}{\partial \log T}[V_\lambda(l,\lambda)+\frac{1}{2}F(y^2)H_\lambda(l,\lambda)]-\frac{m^*}{4m}y^2F'(y^2)H_\lambda(l,\lambda), \tag{A18}$$

Thus the substitution of the results of (A14) and (A18) into (2.7) plus some further straightforward differentiations gives via (6.3) an explicit expression for the internal energy, which together with (2.6) also gives an explicit expression for the entropy.

APPENDIX B: THE COULOMB-OSCILLATOR EQUATION

The following Schrödinger equation arises in Sections V and VI (for $\vec{k}=\vec{0}$) when the many-body effects are taken into account in the manner that we have proposed.

$$-\frac{\hbar^2}{2m}\nabla^2\phi(\vec{r})-\left(\frac{e^2}{r}+ar^2\right)\phi(\vec{r})=E\phi(\vec{r}) \tag{B1}$$

This equation can be separated in spherical coordinates in the usual way to yield the radial equation,

$$-\frac{\hbar^2}{2m}\left(\frac{1}{r^2}\frac{d}{dr}r^2\frac{d}{dr}-\frac{l(l+1)}{r^2}\right)R_l(r)-\left(\frac{e^2}{r}+ar^2\right)R_l(r)=ER_l(r), \tag{B2}$$

with the boundary conditions $R_l(0)$ is finite and

$$R_l(r_b)=0,\ \ l \text{ odd}, \quad R_l'(r_b)=0,\ \ l \text{ even}. \tag{B3}$$

If we use the notation

$$A=-l(l+1), \quad B=\frac{2me^2r_b}{\hbar^2}, \quad C=\frac{2mEr_b^2}{\hbar^2}, \quad D=\frac{2mar_b^4}{\hbar^2}, \quad \text{and} \quad \rho=\frac{r}{r_b}, \tag{B4}$$

then (B2) becomes,

$$\rho^2\frac{d^2R_l(\rho)}{d\rho^2}+2\rho\frac{dR_l(\rho)}{d\rho}+(A+B\rho+C\rho^2+D\rho^4)R_l(\rho)=0. \tag{B5}$$

If we make the usual substitution,

$$R_l(\rho)=u_l(\rho)/\rho, \tag{B6}$$

then (B5) reduces to,

$$\rho^2 \frac{d^2 u_l(\rho)}{d\rho^2} + (A + B\rho + C\rho^2 + D\rho^4) u_l(\rho) = 0, \tag{B7}$$

where now $u_l(0) = 0$ and (B3) becomes,

$$u_l(1) = 0, \;\; l \text{ odd}, \quad u_l'(1) = u_l(1), \;\; l \text{ even}. \tag{B8}$$

We now have the degeneracy of the $2l+1$ m states for each solution of the radial equation. For both the Coulomb potential, and the harmonic oscillator ($a < 0$) potentials in an infinite cell, there is further eigenvalue degeneracy. If we substitute the series expansion,

$$u_l(\rho) = \rho^\nu \sum_{j=1}^{\infty} a_j \rho^j \tag{B9}$$

into (B8), then the indicial equation implies that $\nu = l+1$ or $\nu = -l$. The second case is ruled out by the boundary conditions, so we select the first case. Thus we get the recursion relations,

$$a_j = 0, \; j < 0, \quad a_0 = 1, \quad a_j = -\left[j^2 + (2l+1)j\right]^{-1} \left(B a_{j-1} + C a_{j-2} + D a_{j-4}\right), \; j > 0. \tag{B10}$$

A straightforward analysis indicates that the a_j decrease like $(j!)^{-\frac{1}{2}}$ when $D \neq 0$, so this series converges for all finite ρ. [For $a > 0$ the regular solution oscillates very quickly like $\exp(\frac{1}{2} i \sqrt{D} \rho^2)$, for large ρ, but this feature is not of concern to us here as we are only considering the range $0 \leq \rho \leq 1$.] For the given the values of B and D, the value of C must be adjusted to satisfy the boundary conditions. For the case of (6.2), $D = \frac{1}{2} F(y^2) B$ and $B = (3\sqrt{\pi}/\zeta)^{\frac{2}{3}} y^2$.

In order to implement our approximation scheme to include the effects of the operator $H' = -(i\hbar^2/m)\vec{k}\cdot\vec{\nabla}$ for the Coulomb-oscillator equation, we need to consider the degeneracy, and near-degeneracy structure of the eigenvalues. I have computed them numerically by the same methods as used in Sec. IV. The first observation is that for the higher energies, the states for which $s + [(l+1)/2]$ is a constant are nearly degenerate, as we also saw for the

ideal gas according to equation (4.17), where again s is the level number and l is the angular momentum index. The second observation, is that when the system is sufficiently dilute, the very lowest levels follow the degeneracy pattern of the Coulomb problem. That is to say, the states for which $s + l$ is a constant are very nearly degenerate. There is a fairly sharp transition in the eigenvalue structure as it jumps from one regime to the other. If σ is the highest level in the Coulomb regime for $l = 0$, then this jump occurs between the levels σ and $\sigma + 1$ for $l = 0$. The marker for σ is the condition that the energy level gap $E_{0,\sigma+1} - E_{0,\sigma}$ is a relative minimum among the energy gaps. There then remains a number of (l, λ) states which are in neither regime but lie in the jump. I call them jumper states. There are $\sigma(\sigma - 1)/2$ of them, or when the degeneracy of the $2l + 1$ m-states is taken into account, there are $\sigma(\sigma - 1)(2\sigma + 1)/2$ of them. Specifically, they are the states for which

$$\max(\sigma - l + 1, 1) \leq \lambda \leq \sigma - \left[\frac{l+1}{2}\right], \tag{B11}$$

holds, and we call the set of (l, λ)'s the set $\mathcal{J}$. I observe that that all the jumper states lie in a fairly narrow band of energy, so in line with our approximation in Sec. IV, I will treat them as nearly degenerate. As an illustration in Fig. 12, I show a sample of the structure for $D = \frac{1}{2}B$ (its maximum value) for hydrogen at a compression of 4×10^{-4} times its normal density. The Coulomb-like states are very close to being degenerate (on this scale). The ideal-gas-like states in the low levels show noticeable variation within our nearly degenerate groups, as was also the case for the ideal-gas states tabulated in Table I. The shift between the $F = 0$ case and the $F = 1$ case displayed here is imperceptible for the Coulomb-like states (on this scale) and for the ideal-gas-like states is about one or two dot widths. For intermediate compressions, the low-lying states are noticeably effected by the F corrections but the higher states not so much. For high compressions (for example, 20 times normal densities) the effect of the F correction is not visible on a plot similar to Fig. 12. The effective mass correction only effects ζ and not y. Since $C = (3\sqrt{\pi}/\zeta)^{\frac{2}{3}}(E/kT)$, the value of E/kT is just that for the same value of y and a different value of ζ. Thus the degeneracy structure of the eigenvalue spectrum is not affected by the mass correction, although the

values themselves of course are.

We illustrate in Fig. 13 some of the eigenvalues for the Coulomb potential in the case of a compression of 0.2 times normal liquid hydrogen density. The dotted line connects the eigenvalues for which $s + \left[\frac{l+1}{2}\right] = 27$. This identification corresponds to that for the ideal gas for a set of nearly degenerate states. It is to be observed that, relative to the eigenvalue spacing, these states are nearly degenerate. A little even-odd fluctuation can be seen.

FIGURES

FIG. 1. The pressure of the spherical cellular model of an ideal gas divide by the pressure of the ideal Fermi gas versus ζ, the deBroglie density. The solid line is for (4.25) and the dashed line is for (4.23). The dotted line is for a ratio of unity and is put in for reference.

FIG. 2. The average value of ion-electron attractive energy as computed in the ensemble determined by the spherical cellular model of the ideal Fermi gas.

FIG. 3. The ratio of the electron pressure for hydrogen to the ideal electron gas pressure plotted versus ζ the de Broglie density along the $T = 1000$ eV isotherm.

FIG. 4. The ratio of the electron gas pressures for hydrogen at $T = 2,\ 5,\ 10$, and 100 ev. to the pressure computed in the Thomas-Fermi model at the same volume and zero temperature. There is a dotted line included at unit ratio to guide the eye. The volume is in cm^3 per gram.

FIG. 5. The total pressure for hydrogen in megabars as a function of the volume in cc. per gram for the $T = 1.5$ eV isotherm. The solid curve represents out model, and the dashed curve omits the many-body terms. The dotted line shows the cross-over pressure as computed by the Maxwell construction for the solid curve. The line of short dashes shows it for the dashed curve.

FIG. 6. The total pressures for hydrogen in megabars versus the volume in cm^3 per gram for the following isotherms. In descending order, $T = 10,\ 5,\ 2,\ 1.83,\ 1.7,\ 1.5,\ 1.0,\ 0.5$, and 0.1 eV.

FIG. 7 The phase boundary of the cellular model of hydrogen in the volume-temperature plane and the pressure-temperature plane. The dot is the critical point.

FIG. 8 The ratio of the total pressure to that of the sum of the pressures due to non-interaction electrons and protons along the phase boundary. The critical point is indicated by a dot. The expected value for atomic hydrogen is indicated by a dotted line.

FIG. 9 The energy of the electron in the spherical cellular model of hydrogen at a temperature of 0.5 eV as a function of volume. The energy is in electron volts and the volume in cm^3 per gram. The dotted line indicates the binding energy of the electron in atomic hydrogen. The large dots mark the boundaries of the two phase region. The dashed curve is the result with no many-body terms.

FIG. 10 The ratio of the energy of the electron to the energy of an electron in an ideal electron gas as a function of density for the $T = 10$ eV isotherm. The density is in grams/cm^3. .

FIG. 11 The ratio of the electron pressure in the spherical cellular model of hydrogen to the pressure of an ideal electron gas for the four densities which are the result of compression of 1, 0.1, 0.01, and 0.001 of a system of the density of liquid hydrogen. The temperature is in electron volts.

FIG. 12 Some of eigenvalues in units of 4 Rydbergs for the Coulomb oscillator potential of (B7) with $D = \frac{1}{2}$, and $B = (3\sqrt{\pi}/\zeta)^{\frac{2}{3}} y^2$. $(F = 1)$ The jumper states are connected by solid lines. The Coulomb-like states are connected in groups by dotted lines, and lie below the jumper states. The ideal-gas-like states are also connected in groups by dotted lines but lie above the jumper states.

FIG. 13 Some of the eigenvalues in units of 4 Rydbergs for the Coulomb potential for hydrogen. The dotted line connects the eigenvalues characterized by $27 = s + \left[\frac{l+1}{2}\right]$.

TABLES

TABLE I. The values of $p_{l,\lambda}$ in units of π. $\omega = \lambda + [(l+1)/2]$ where $[a]$ is the greatest integer not exceeding a.

$l \setminus \omega$	0	1	2	3	4
0	0.0000	1.4303	2.4590	3.4709	4.4775
1		1.4303	2.4590	3.4709	4.4775
2		1.0638	2.3205	3.3785	4.4074
3			2.2243	3.3159	4.3602
4			1.7974	3.1323	4.2321

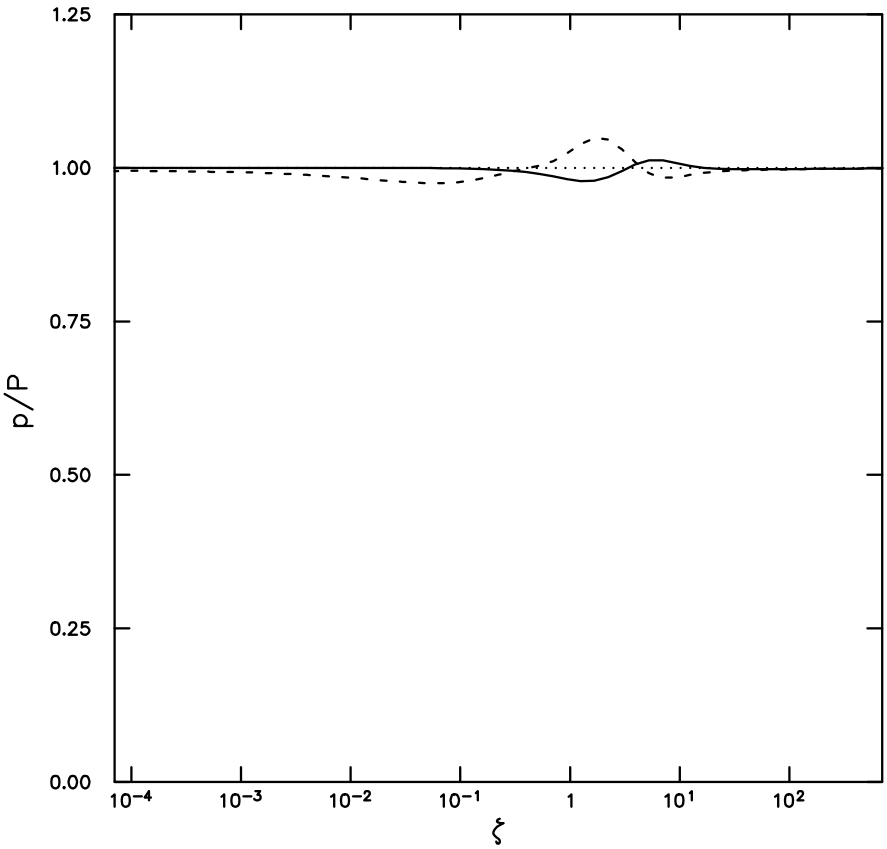

Figure 1

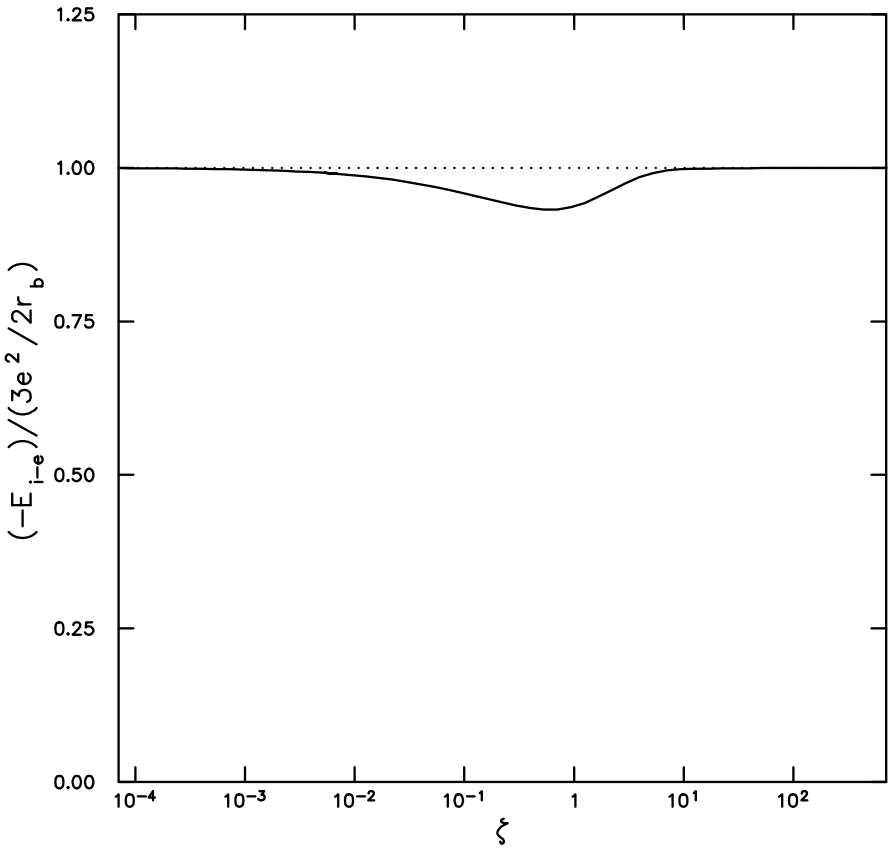
1.25
1.00
0.75
0.50
0.25
0.00
$(-E_{i-e})/(3e^2/2r_b)$
10^{-4}
10^{-3}
10^{-2}
10^{-1}
1
10^{1}
10^{2}
ζ

Figure 2

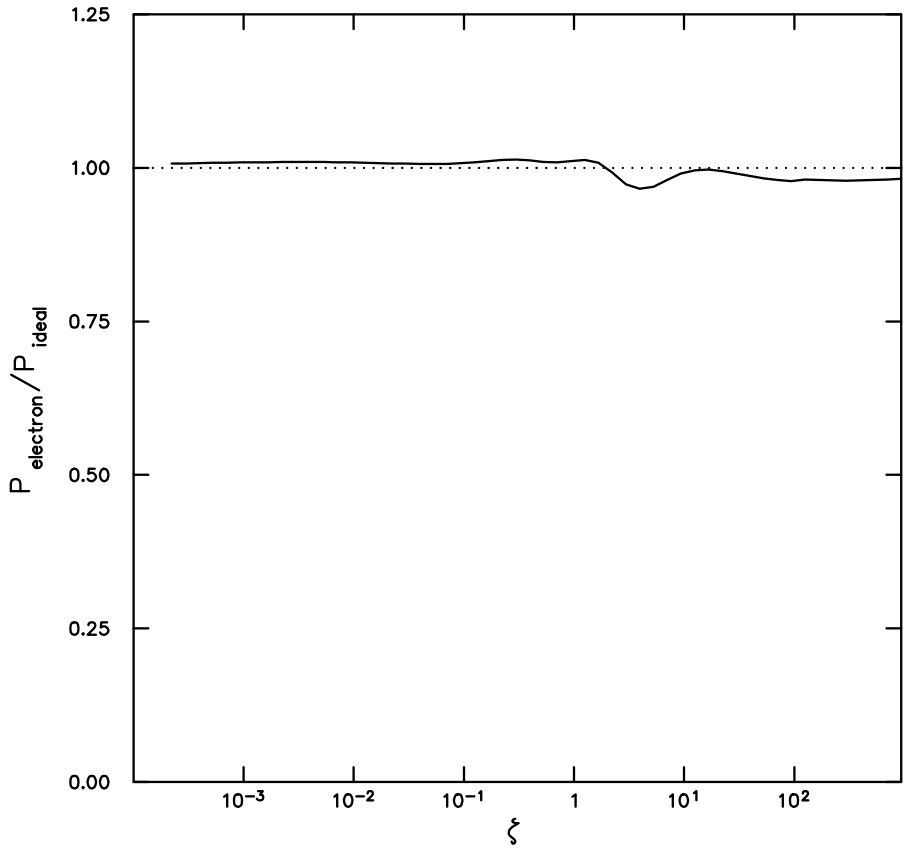
1.25
1.00
0.75
0.50
0.25
0.00
P electron/P ideal
10−3
10−2
10−1
1
101
102
ζ

Figure 3

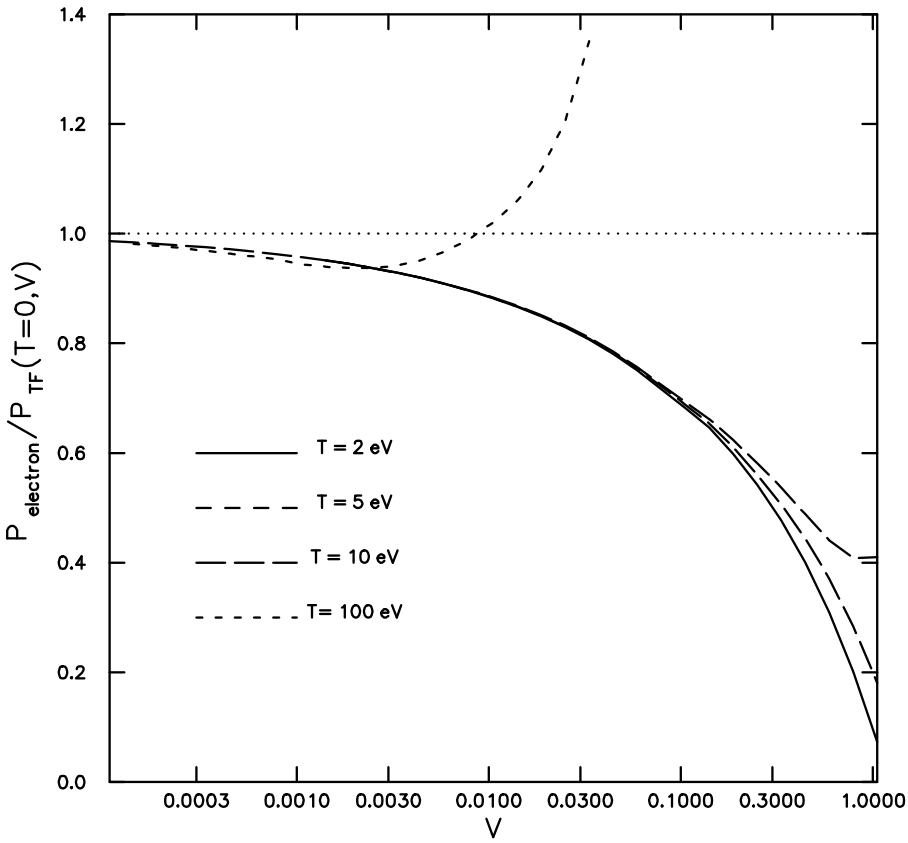
1.4
1.2
1.0
0.8
0.6
0.4
0.2
0.0
P electron/P TF(T=0,V)
T = 2 eV
T = 5 eV
T = 10 eV
T= 100 eV
0.0003
0.0010
0.0030
0.0100
0.0300
0.1000
0.3000
1.0000
V

Figure 4

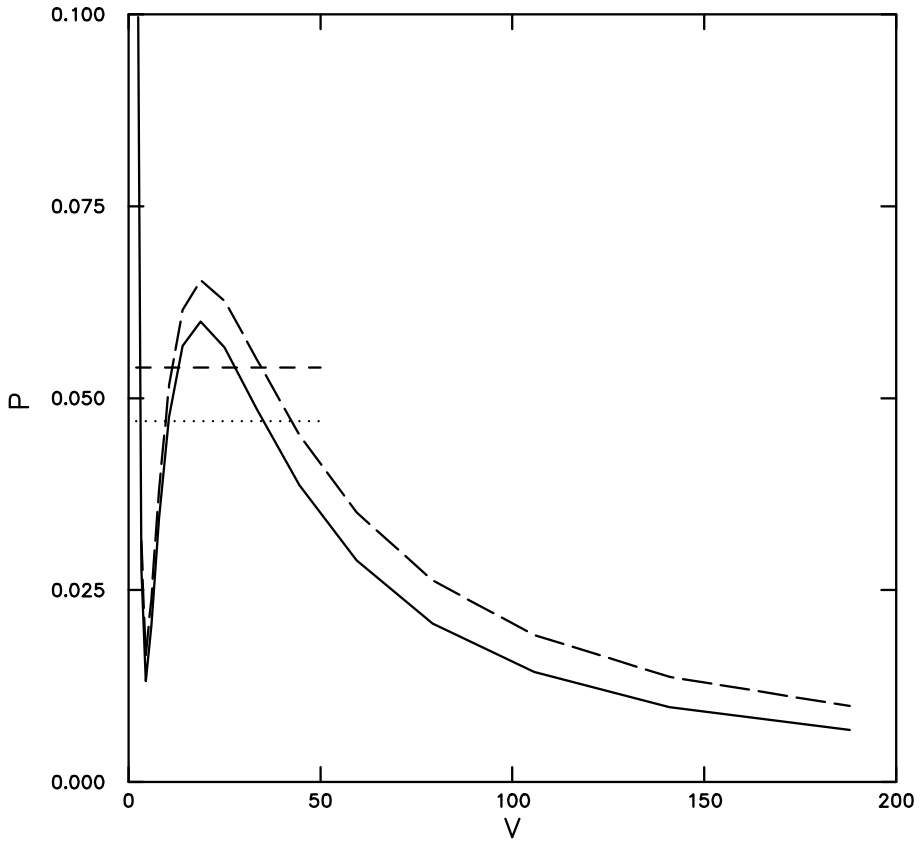

Figure 5

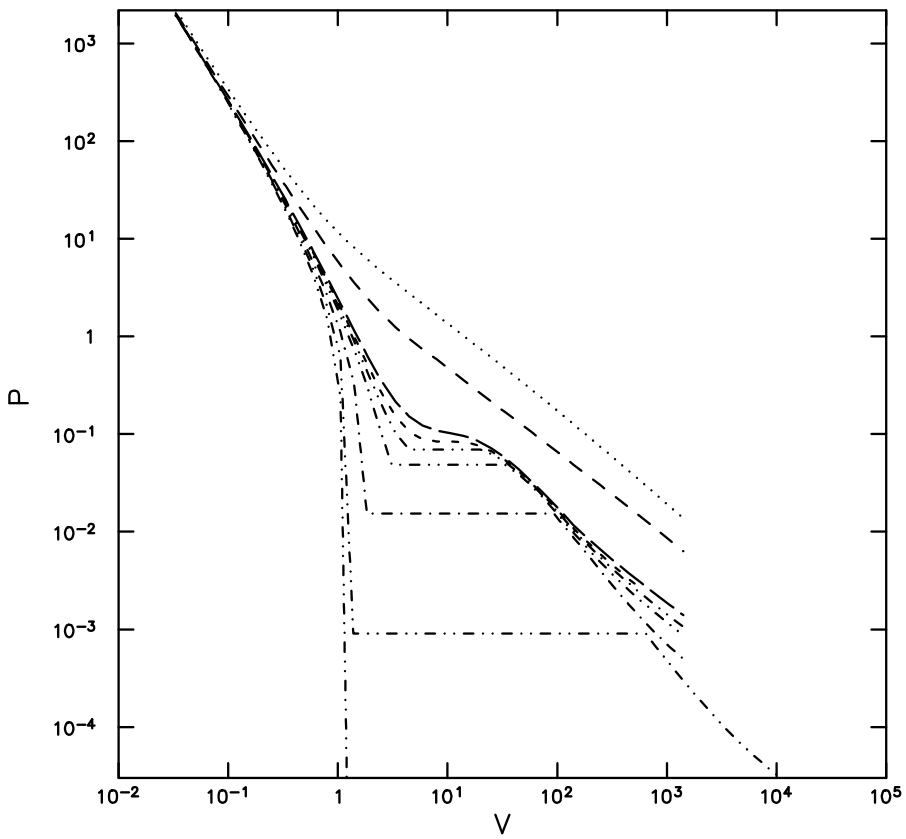

Figure 6

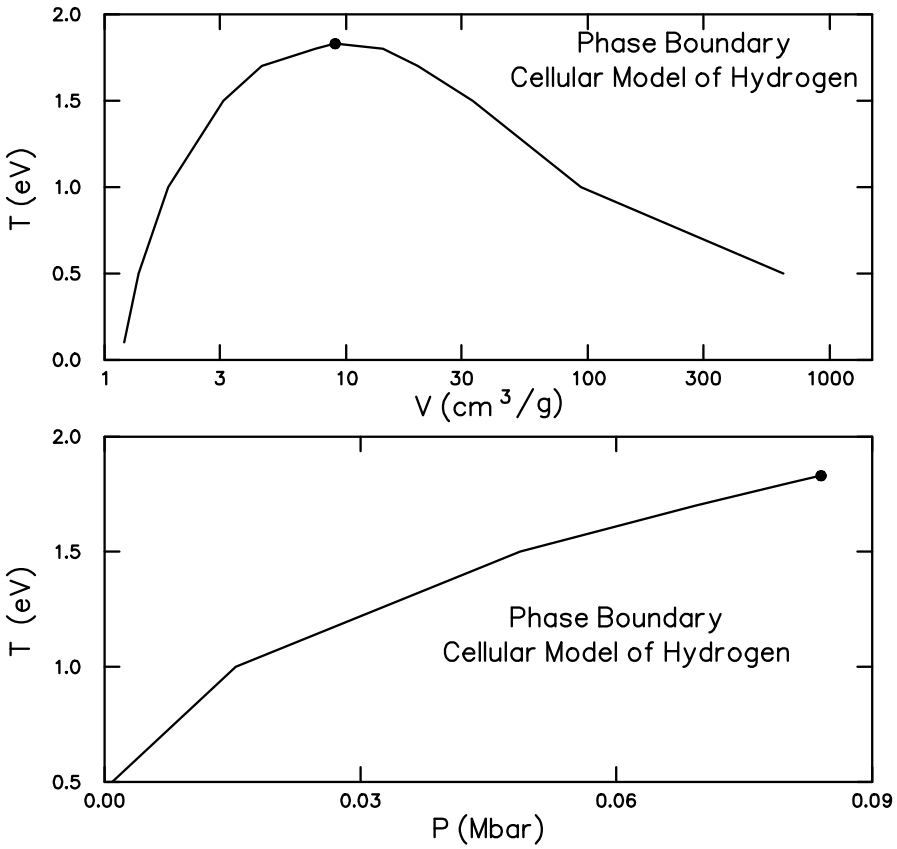
Phase Boundary
Cellular Model of Hydrogen
T (eV)
V (cm 3/g)
2.0
1.5
1.0
0.5
0.0
1
3
10
30
100
300
1000
Phase Boundary
Cellular Model of Hydrogen
T (eV)
P (Mbar)
2.0
1.5
1.0
0.5
0.00
0.03
0.06
0.09

Figure 7

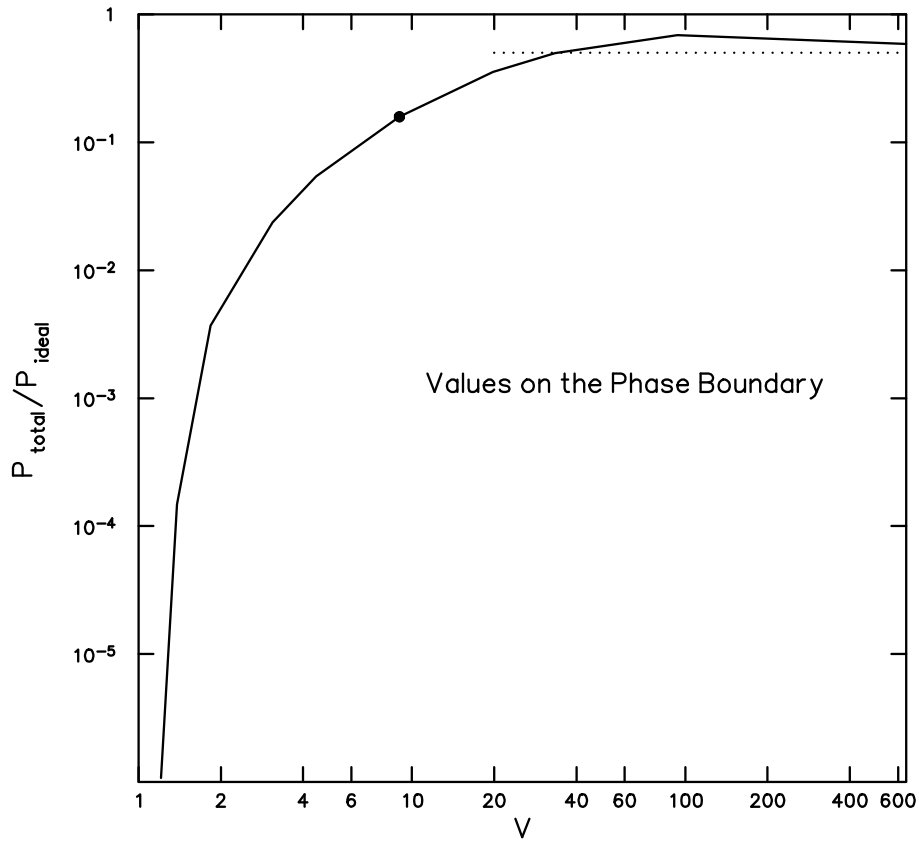
1
10−1
10−2
10−3
10−4
10−5
P total/P ideal
Values on the Phase Boundary
1
2
4
6
10
20
40
60
100
200
400
600
V

Figure 8

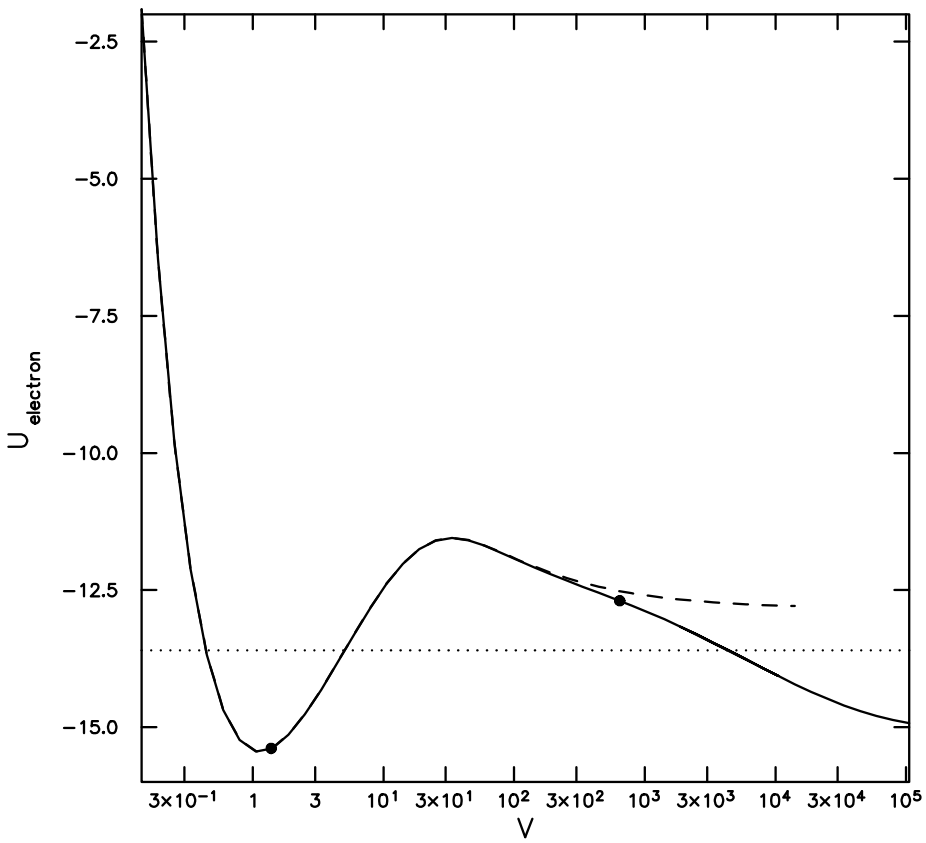
−2.5
−5.0
−7.5
−10.0
−12.5
−15.0
U electron
3×10⁻¹
1
3
10¹
3×10¹
10²
3×10²
10³
3×10³
10⁴
3×10⁴
10⁵
V

Figure 9

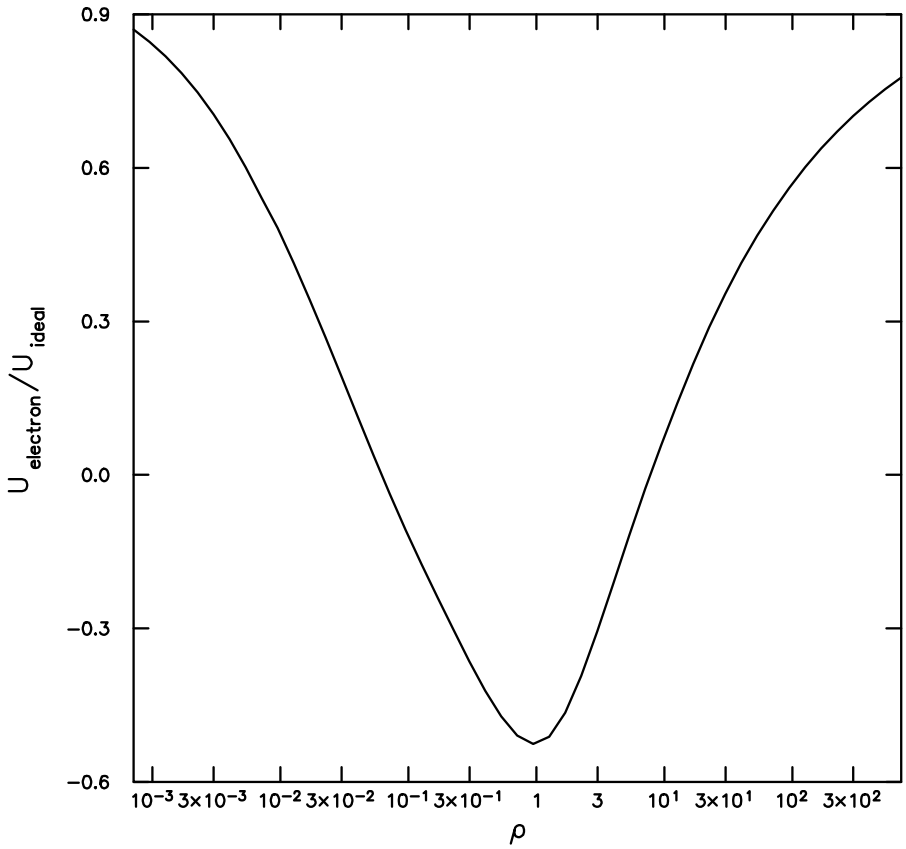
0.9
0.6
0.3
0.0
−0.3
−0.6
U electron/U ideal
10−3 3×10−3 10−2 3×10−2 10−1 3×10−1 1 3 101 3×101 102 3×102
ρ

Figure 10

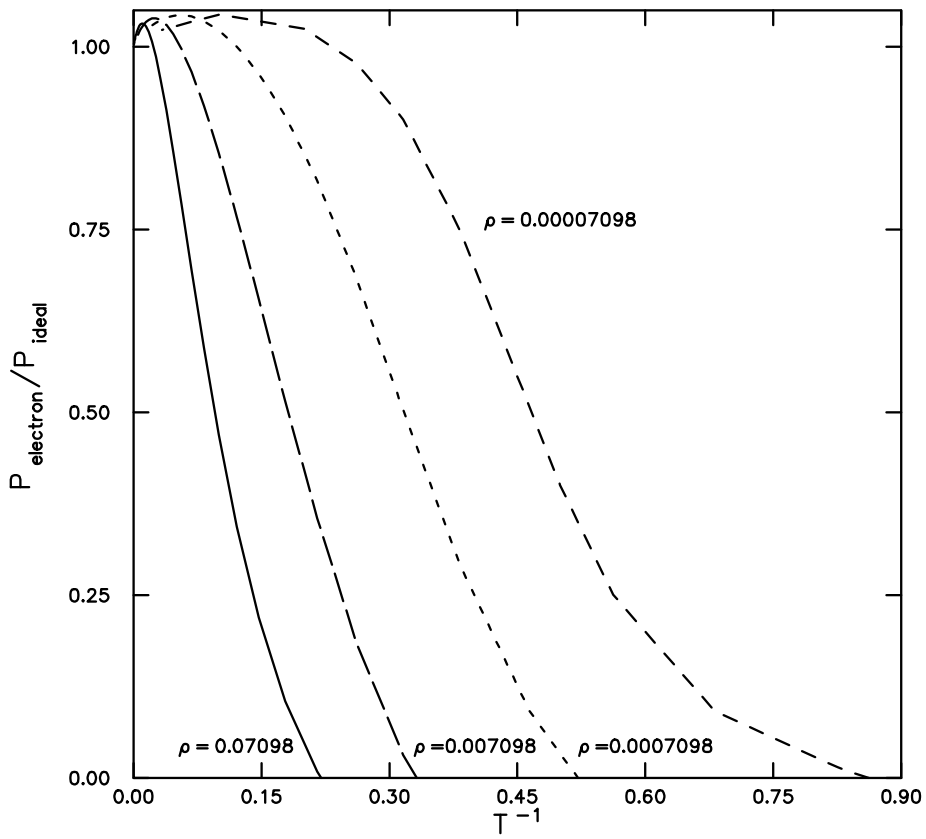
1.00
0.75
0.50
0.25
0.00
0.00
0.15
0.30
0.45
0.60
0.75
0.90
P electron/P ideal
T −1
ρ = 0.00007098
ρ = 0.07098
ρ =0.007098
ρ =0.0007098

Figure 11

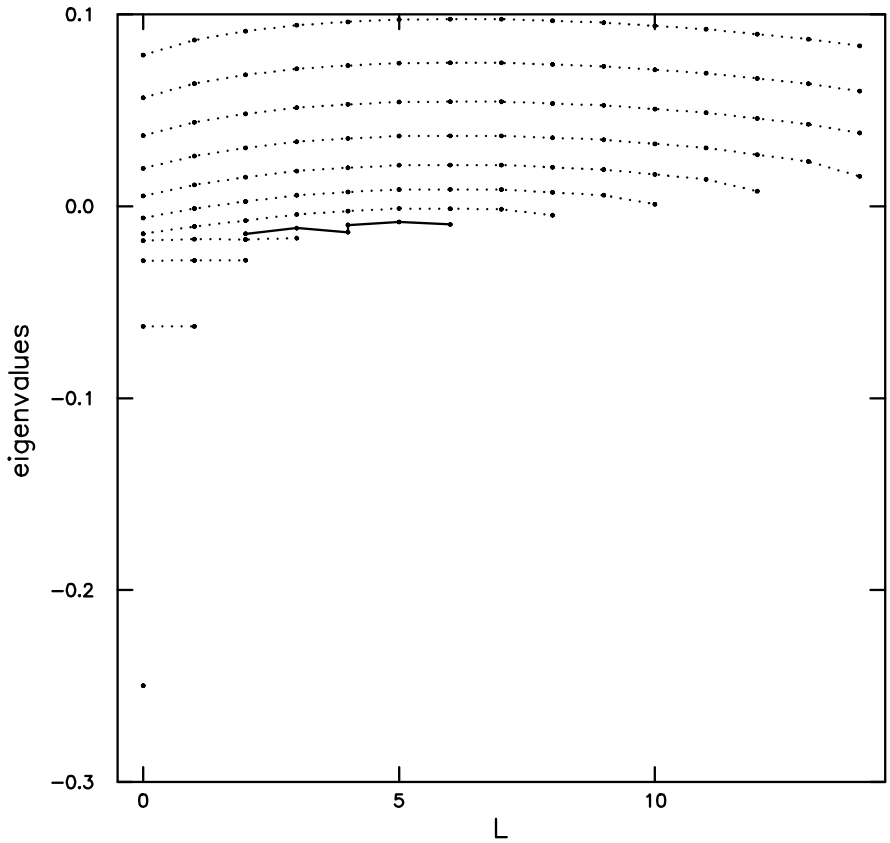

Figure 12

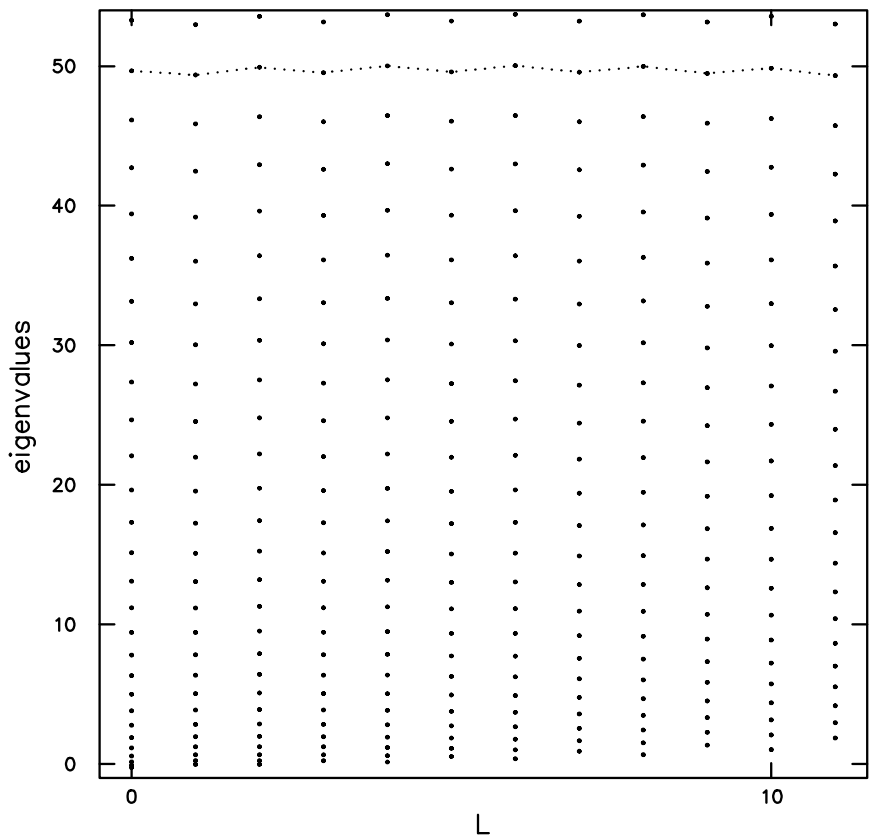

Figure 13